Data Gathering Optimization by Dynamic Sensing and Routing in Rechargeable Sensor Networks

Yongmin Zhang, *Student Member, IEEE*, Shibo He, *Member, IEEE*, and Jiming Chen, *Senior Member, IEEE*

***Abstract*—In rechargeable sensor networks (RSNs), energy harvested by sensors should be carefully allocated for data sensing and data transmission to optimize data gathering due to time-varying renewable energy arrival and limited battery capacity. Moreover, the dynamic feature of network topology should be taken into account, since it can affect the data transmission. In this paper, we strive to optimize data gathering in terms of network utility by jointly considering data sensing and data transmission. To this end, we design a data gathering optimization algorithm for dynamic sensing and routing (DoSR), which consists of two parts. In the first part, we design a balanced energy allocation scheme (BEAS) for each sensor to manage its energy use, which is proven to meet four requirements raised by practical scenarios. Then in the second part, we propose a distributed sensing rate and routing control (DSR2C) algorithm to jointly optimize data sensing and data transmission, while guaranteeing network fairness. In DSR2C, each sensor can adaptively adjust its transmit energy consumption during network operation according to the amount of available energy, and select the optimal sensing rate and routing, which can efficiently improve data gathering. Furthermore, since recomputing the optimal data sensing and routing strategies upon change of energy allocation will bring huge communications for information exchange and computation, we propose an improved BEAS to manage the energy allocation in the dynamic environments and a topology control scheme to reduce computational complexity. Extensive simulations are performed to demonstrate the efficiency of the proposed algorithms in comparison with existing algorithms.**

***Index Terms*—Data sensing, dynamic topology, energy allocation, energy harvesting, rechargeable sensor networks, routing.**

I. Introduction

DATA gathering has been a fundamental issue in Wireless Sensor Networks (WSNs) [1], [2]. It mainly consists of two steps: i) data sensing, which decides the sensing rate of each sensor to well reconstruct the physical information, and ii) data transmission, which is concerned with how to transmit sensory data to sink node. In order to reconstruct the physical information with high accuracy at sink node, both data sensing and data transmission should be optimized. As battery-powered sensors are not feasible for long-term applications, energy harvesting technologies have been recently introduced to achieve the goal of perpetual network operation [3]–[6].

Data gathering optimization was previously addressed in battery-powered WSNs [7]–[11]. A popular approach is to jointly optimize data sensing and data transmission globally by using cross-layer optimization. As the energy budget of each sensor is given initially, the problem can be formulated as a deterministic optimization problem. However, energy arrival at each sensor is intrinsically stochastic in RSNs. To optimize data gathering, sensors have to dynamically determine their sensing and transmission strategies in order to fully utilize the harvested energy according to the instant profile of energy arrival. These unique features make data gathering in RSNs a radically new and challenging problem, which is far from data gathering in battery-powered WSNs.

In this paper, we seek to optimize data gathering in RSNs by jointly considering data sensing and data transmission. Existing works either assumed a static network topology or considered data sensing and data transmission independently. For example, Liu *et al.* proposed a distributed algorithm to jointly compute a routing structure and a high lexicographic rate assignment, provided that the available logical links are predetermined [12]. In practice, according to the amount of available energy, each sensor can adaptively adjust its transmit energy consumption within a certain range during network operation to improve the efficiency of data gathering by selecting optimal sensing rate and routing. Therefore, the dynamic feature of network topology should be taken into account to improve the efficiency of data gathering. In addition, since sensors should communicate with each other to compute the optimal data sensing and data transmission upon different energy allocation,[1] changing the energy allocation frequently may bring extra energy cost for communication and computation. Thus, the extra energy cost, as well as the computational complexity, should be taken into consideration.

The objective of this paper is to design an algorithm for data gathering optimization via dynamic sensing and routing (DoSR) that can maximize data gathering (in the form of utility) by jointly optimizing energy allocation, data sensing and data transmission for each sensor while taking the dynamic

Manuscript received March 11, 2014; revised September 20, 2014; accepted March 30, 2015; approved by IEEE/ACM TRANSACTIONS ON NETWORKING Editor L. Ying. Date of publication June 01, 2015; date of current version June 14, 2016. This research was supported in part by NSFC under grants 61222305, NCET-11-0445, National Program for Special Support of Top-Notch Young Professionals, and the Fundamental Research Funds for the Central Universities under grant 2015FZA5011. *(Corresponding author: Jiming Chen.)*

The authors are with State Key Laboratory of Industrial Control Technology, Department of Control Science and Engineering, Zhejiang University, Hangzhou 310027, China (e-mail: ymzhang@zju.edu.cn; s18he@zju.edu.cn; jmchen@iipc.zju.edu.cn).

This paper has supplementary downloadable material available at http://ieeexplore.ieee.org, provided by the authors.

Color versions of one or more of the figures in this paper are available online at http://ieeexplore.ieee.org.

Digital Object Identifier 10.1109/TNET.2015.2425146

[1]Energy allocation is an energy management scheme, which is used to decide the upper bound of the energy use in each slot.

1063-6692 © 2015 IEEE. Personal use is permitted, but republication/redistribution requires IEEE permission.
See http://www.ieee.org/publications_standards/publications/rights/index.html for more information.

feature of network topology into consideration. Specifically, our contributions are summarized as follows:

- We propose a balanced energy allocation scheme (BEAS) to manage the energy use adaptively according to the battery level and the amount of harvested energy for each sensor, so that all sensors can efficiently utilize the harvested energy.
- Based on BEAS, we design a distributed sensing rate and routing control (DSR2C) algorithm by employing dual decomposition method and sub-gradient method. We theoretically investigate the performance of DSR2C, showing that DSR2C converges to the optimal sensing rate and routing for the data gathering problem.
- We propose an improved BEAS scheme to manage the energy allocation that can prevent the decrease of network utility due to extra energy cost incurred by the change of energy allocation, and a topology control scheme to manage the established logical links to reduce computational complexity.
- Extensive simulations based on real experimental data are performed to demonstrate the efficiency of the proposed algorithms.

The remainder of this paper is organized as follows. We introduce the related work in Section II and describe the network model and problem formulation in Section III. Then, a balanced energy allocation scheme (BEAS) for each sensor to manage its energy use efficiently is proposed and a distributed sensing rate and routing control (DSR2C) algorithm to find the optimal sensing rate and routing is designed in Section IV. We propose an improved BEAS and a topology control scheme in Section IV. We evaluate the performance of the proposed algorithms in Section V. We conclude this work in Section VI.

II. Related Work

Recently, there are many works on optimal data sensing and routing in WSNs. In [7], Hua *et al.* presented a smoothing approximation function of network lifetime maximization problem by integrating date aggregation with underlying routing scheme, and proposed a distributed gradient algorithm accordingly. In [8], He *et al.* presented a network lifetime maximization problem by jointly considering routing layer, physical layer and MAC layer. An efficient heuristic algorithm, JRPRA, was designed, which could obtain a close-to-optimal solution. In [13], Nair *et al.* formulated the network utility maximization problem as a nonconvex function and presented a distributed and iterative algorithm to attain globally optimal transmission rate and routing, respectively. In [14], Long *et al.* formulated the throughput maximization and energy efficiency problem as a cross-layer design problem, and then designed a joint congestion control, random access and power control algorithm. In [15], Xi *et al.* aimed to minimize the sum of link costs and proposed an optimal power control, routing and congestion control algorithm. However, all of the aforementioned works focus on battery-powered WSNs, which cannot be directly applied to RSNs.

There are several works that aim to optimize energy management, data sensing and routing in RSNs. In [16], Chen *et al.* investigated the utility maximization problem for the rechargeable sensor networks and developed a joint energy allocation and routing algorithm, which is a low-complexity online solution. In [17], Liu *et al.* focused on network utility maximization and perpetual network operation, and developed a QuickFix algorithm to compute the optimal sampling rate and route, and a SnapIt algorithm to adjust the sampling rate. In [18], Lin *et al.* proposed an integrated admission control and routing framework, and designed routing algorithms to optimally utilize the available energy. In [19], Zhang *et al.* proposed a distributed algorithm to jointly optimize energy management, data sensing and routing for sensors to maximize overall network utility. In [20], Joseph *et al.* designed a joint optimal power control, routing and scheduling algorithm to ensure that the network resources can be fairly utilized. In [21], Zhao *et al.* studied the network utility maximization and proposed a distributed algorithm to adjust data rates, link scheduling and routing according to the up-to-date energy replenishing status of the sensors. Most of the aforementioned works assume that a static network topology and the transmit energy consumption for each sensor is fixed initially, which may degrade the network performance.

By taking into account time-varying characteristic of network topology, our goal is to maximize the data gathering by jointly optimizing the optimal energy allocation, data sensing and data transmission. Thus our work is different from existing works and has the potential to significantly improve the network performance. In addition, we proposed an improved energy allocation scheme to reduce the extra energy cost and a topology control scheme to reduce computational complexity for the sensors to obtain the optimal data sensing and data transmission.

III. Network Model and Problem Formulation

We consider a rechargeable sensor network, with N rechargeable sensors (including one sink node). Each sensor consists of a solar cell, a rechargeable battery and a wireless module. All the rechargeable sensors can harvest energy from solar and reserve them in battery for future use. As typically assumed [12], [22], the sink node is powered by unconstrained power source and each sensor harvests less energy than what it consumes. Sensors can transmit their sensory data to the sink node through the logical links in a multi-hop manner. Furthermore, one sensor only relays data for other sensors, which are farther from the sink node.

A summary of notations used in this paper is given in Table I.

A. Energy Management Model

Each day is one period of solar energy harvesting process, which can be divided into T slots. Let $\rho_{i,t}$ and $A_{i,t}$ denote the total amount of harvested energy and energy allocation for sensor i at slot t, $t = 1, 2, \ldots, T$, respectively. We assume that each sensor can estimate $\rho_{i,t}$ with high accuracy, which can be inferred from historical information by existing works [23], [24]. Let $B_{i,t}$ denote the remaining energy of sensor i at slot t and $B_i^{\max}$ the maximum battery level of sensor i. $B_{i,t}$ is given by

$$B_{i,t+1} = [B_{i,t} + \rho_{i,t} - A_{i,t}]_0^{B_i^{\max}} \tag{1}$$

TABLE I
NOTATION DEFINITIONS

Symbol	Definition
N	The total number of sensors in the network
T	The total amount of slots in each cycle
t	The t-th slot, $t = 1, 2, \cdots, T$
i (k)	Sensor (excluding sink node) i (k)
j (l)	Sensor or sink node j (l)
$B_{i,1}$	The initial battery level of sensor i
$B_{i,t}$	The battery level of sensor i at slot t
B_i^{max}	The maximum battery level of sensor i
$\rho_{i,t}$	The amount of energy harvested by sensor i at slot t
$A_{i,t}$	The energy allocation of sensor i at slot t
$o_{i,t}$	The surplus variable that denotes the amount of harvested energy that can not be stored by the rechargeable battery
e_i^{sn}	The average energy cost for sensor i to sense one unit data from the enviroment
e_{ij}^{tr}	The average energy cost for sensor i to transmit one unit data sensor j
e_i^{re}	The average energy cost for sensor i to receive one unit data from other sensors
$x_{i,t}$	The total amount of data sensed by sensor i at slot t
$f_{ij,t}$	The total amount of data transmitted from sensor i to sensor j using logical link (i, j) at slot t
$P_{i,t}$	The energy consumption for sensor i at slot t

where $[\cdot]_0^{B_i^{\max}} = \max(0, (\min(\cdot, B_i^{\max}))$. Obviously, the amount of energy allocation $A_{i,t}$ for sensor i at slot t should satisfy

$$A_{i,t} \leq B_{i,t} + \rho_{i,t}. \tag{2}$$

Moreover, in order to establish sustainable operation, sensors cannot consume more energy than what they can collect [25], [26], i.e.,

$$\sum_{t=1}^{T} A_{i,t} \leq \sum_{t=1}^{T} \rho_{i,t}. \tag{3}$$

Let surplus variable $o_{i,t}$ denote the amount of harvested energy that cannot be stored in the rechargeable battery by sensor i, i.e.,

$$o_{i,t} = [B_{i,t} + \rho_{i,t} - A_{i,t} - B_i^{\max}]^+ \tag{4}$$

where $[\cdot]^+ = \max(0, \cdot)$. Obviously, a smaller $o_{i,t}$ means that sensor i utilizes the harvested energy more efficiently.

B. Energy Consumption Model

We only consider the energy consumption for transmitting, receiving and sensing in this paper. Let e_{ij}^{tr}, e_i^{re}, and e_i^{sn} denote the average energy cost at sensor i for transmitting one unit data to sensor j, receiving and sensing one unit data, respectively. For sensor i transmitting one unit data over distance r_{ij} using the logical link (i, j), the minimal transmit energy consumption E_{ij}, $E_{ij} \in \boldsymbol{E}$, can be given by

$$E_{ij} = \beta + \mu r_{ij}^{\alpha} \tag{5}$$

where β is a distance-independent term, μ is a distance-dependent term and α is the path-loss exponent ($2 \leq \alpha \leq 4$ for the free-space and short-to-medium-range radio communication) [27], [28]. The receive energy consumption for each sensor to receive one unit data from other sensors can be arranged at a certain level. For simplicity, we assume that the signal interference between sensors can be eliminated by underlying MAC layer (e.g., by TDMA or FDMA mechanism). Each sensor can adjust its transmit energy consumption within a certain range to establish a new logical link with another sensor. Thus, the transmit energy consumption, which can be adjusted in $[0, e^{\max}]$, needs to be larger than the minimal transmit energy consumption, i.e.,

$$E_{ij} \leq e_{ij}^{tr} \leq e^{\max}. \tag{6}$$

We use an accessible matrix R to represent the established logical links for the sensors, whose ijth entry is given by

$$R_{ij} = \begin{cases} 1, & \text{if } e_{ij}^{tr} \text{ satisfies constraint (6),} \\ 0, & \text{otherwise.} \end{cases} \tag{7}$$

When the element R_{ij} equals to 1, sensor i can transmit sensory data through the logical link (i, j). Let $\mathbb{O}(i)$ denote the set of sensors that sensor i can directly forward sensory data to, and $\mathbb{I}(i)$ denote the set of sensors that can directly forward sensory data to sensor i. Therefore, if $j \in \mathbb{O}(i)$, the transmit energy consumption for sensor i needs to satisfy $R_{ij} = 1$. Let $x_{i,t}$ denote the total amount of the sensory data sensed by sensor i at slot t, and $f_{ij,t}$ denote the total amount of sensory data that should be transmitted from sensor i to sensor j using the link (i, j) at slot t. Since the sensory data needs to be transmitted to the sink node at slot t so that it can be retrieved timely, the total amount of incoming flow and outgoing flow for sensor i should satisfy flow conservation condition,

$$f_{i,t}^{in} + x_{i,t} = f_{i,t}^{out} \tag{8}$$

where

$$f_{i,t}^{in} = \sum_{k \in \mathbb{I}(i)} f_{ki,t} \quad \text{and} \quad f_{i,t}^{out} = \sum_{j \in \mathbb{O}(i)} f_{ij,t}. \tag{9}$$

The in-network traffic in sensor networks is typically low, thus we assume that the link capacity is large enough to support data transmission [12]. According to the energy consumption model, the total amount of energy consumption $P_{i,t}$ for receiving, transmitting and sensing for sensor i at slot t is

$$P_{i,t} = e_i^{re} \sum_{k \in \mathbb{I}(i)} f_{ki,t} + e_i^{sn} x_{i,t} + \sum_{j \in \mathbb{O}(i)} f_{ij,t} e_{ij}^{tr} \tag{10}$$

which cannot exceed the total amount of the allocated energy for sensor i at slot t, as

$$A_{i,t} \geq P_{i,t}. \tag{11}$$

C. Problem Formulation

Let $U(x_{i,t})$ denote the utility function of sensor i, which is continuously differentiable, increasing and strictly concave. In this paper, we set $U(x_{i,t}) = \log(x_{i,t})$, since it can guarantee the fairness of sensing rate [17], [29], [30]. We aim to maximize the network utility by managing energy allocation, controlling optimal sensing rate and choosing optimal routing, i.e.,

$$Objective \max_{x_{i,t}, f_{ij,t}, e^{tr}_{ij,t}} \sum_i \sum_t U(x_{i,t}) \tag{12}$$

$$s.t.\ f^{in}_{i,t} + x_{i,t} = f^{out}_{i,t}, \quad \forall i,t \tag{13}$$

$$A_{i,t} \geq P_{i,t}, \quad \forall i,t \tag{14}$$

$$e^{tr}_{ij,t} \geq E_{ij}, \quad \forall i,j \in \mathbb{O}(i),t \tag{15}$$

$$A_{i,t} \leq B_{i,t} + \rho_{i,t}, \ \forall i,t \tag{16}$$

$$\sum_{t=1}^{T} A_{i,t} \leq \sum_{t=1}^{T} \rho_{i,t}, \ \forall i,t. \tag{17}$$

Equation (13) is flow conservation constraint, and (14) is energy conservation constraint. Equation (15) is transmit energy consumption constraint, which ensures that the transmit energy consumption needs to be larger than the minimal transmit energy consumption. Equations (16) and (17) are used to guarantee that the energy allocation is reachable and uninterrupted. Note that i denotes a sensor excluding sink node.

Remark: In this problem formulation, we do not take the constraints for the sink node into consideration, due to the following reasons:

- Since the sink node s does not transmit sensory data to other sensors, $f^{out}_{s,t}$ always equals to 0 at each slot t. Hence, sink node does not satisfy the flow conservation constraint.
- Further, all the flows are unidirectional as one sensor only relays data for other sensors, which are farther from sink node. Note that the sink node does not have the energy constraint, i.e., it is connected to the power source. Therefore, there is no variable associated with sink node in the constraint $\sum x_{i,t} = f^{in}_{s,t}$, and this constraint will always hold. In other words, if all the sensors satisfy the flow conservation constraint, $\sum x_{i,t} = f^{in}_{s,t}$ will also be satisfied. In view of this, we omit this constraint for the sink node in our formulation.

It can be observed that problem (12)–(17) is a dynamic problem, since the energy allocation needs to be adjusted according to both remaining energy and harvested energy in the future. To solve the problem (12)–(17), we need to optimize sensing rates $\boldsymbol{x} = \{x_{i,t},\ i = 1,2,\ldots,N,\ t = 1,2,\ldots,T\}$ and flow rates $\boldsymbol{F} = \{f_{ij,t},\ i,j = 1,2,\ldots,N,\ t = 1,2,\ldots,T\}$, which are coupled with the amount of energy allocation, i.e., $\boldsymbol{A} = \{A_{i,t},\ i = 1,2,\ldots,N,\ t = 1,2,\ldots,T\}$. Moreover, each sensor can adjust its transmit energy consumption to establish new logical links for routing selection. Hence, in the next section, we design a DoSR, which consists of an efficient energy allocation scheme and an optimal sensing rate and routing algorithm.

IV. Data Gathering Optimization by Dynamic Sensing and Routing (DoSR)

In this part, we design an algorithm for DoSR, which consists of two schemes, i.e., BEAS and DSR2C. During the operation, DoSR is run dynamically at the beginning of each period and then all sensors follow the decision obtained by DoSR in the rest of the period.

A. Balanced Energy Allocation Schemes

We first focus on the energy allocation for each sensor. Due to the time-varying profile of the harvested energy, it is hard for the rechargeable sensor to provide balanced and fair data service without an efficient energy allocation scheme.

As introduced in [24], an optimal energy allocation scheme should satisfy the following four requirements:

1) Maintain Energy-neutral operation, i.e., (3);
2) Minimize total amount of the wasted harvested energy, i.e., minimize $\max\{o_{i,t}, t = 1,2,\ldots,T\}, \forall i$;
3) Minimize variations in the energy allocation, i.e., minimize $\sum_{t=1}^{T}(A_{i,t} - \pi_{i,t})^2$;
4) Never runs out of energy, i.e., $\min\{\hat{B}_{i,t}, t = 1,2,\ldots,T\} \geq 0, \forall i$, where $\hat{B}_{i,t}$ is given by (19).

In the above, 1) guarantees that each sensor cannot consume more energy than that it can collect, 2) ensures that each rechargeable sensor can well utilize the harvested energy and never misses any recharging opportunity, 3) requires that each sensor use its energy as smooth as possible, 4) guarantees that each sensor never runs out of energy, since running out of energy means the interruption of the continuous sensing.

We propose a balanced energy allocation scheme (BEAS), which can satisfy the aforementioned four requirements. Specifically, let

$$\pi_{i,t} = \frac{1}{T}\sum_{t=1}^{T} \rho_{i,t}. \tag{18}$$

Since the total amount of utility is an increasing and concave function of energy allocation (given in Theorem 4), it can be found that if the battery capacity is large enough, the energy allocation for sensor i in all slots will equal to $\pi_{i,t}$. Thus, we take the $\pi_{i,t}$ as an initial energy allocation, i.e., $A_{i,t} = \pi_{i,t}, \forall t$.

Let $\hat{B}_{i,t} \in (-\infty, \infty)$ denote the virtual battery level, which is a dummy variable for ease of presentation. We have

$$\hat{B}_{i,t+1} = \hat{B}_{i,t} + \rho_{i,t} - A_{i,t}. \tag{19}$$

Then, we design BEAS for each sensor to manage its energy use in an efficient way, which guarantees $0 \leq \hat{B}_{i,t} \leq B^{\max}$.

The initial $A_{i,t}$ is set to be $\pi_{i,t}$, and the virtual battery level will be updated according to (19). Then we define an upper and a lower bound, denoted by $\hat{B}^{up}_i$ and $\hat{B}^{low}_i$, respectively, i.e.,

$$\hat{B}^{up}_i = \max\{\hat{B}_{i,t+1},\ t = 1,2,\ldots,T\}, \tag{20}$$

$$\hat{B}^{low}_i = \min\{\hat{B}_{i,t+1},\ t = 1,2,\ldots,T\}. \tag{21}$$

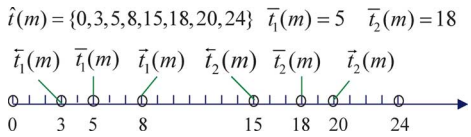

Fig. 1. An illustration of $\hat{t}(m)$.

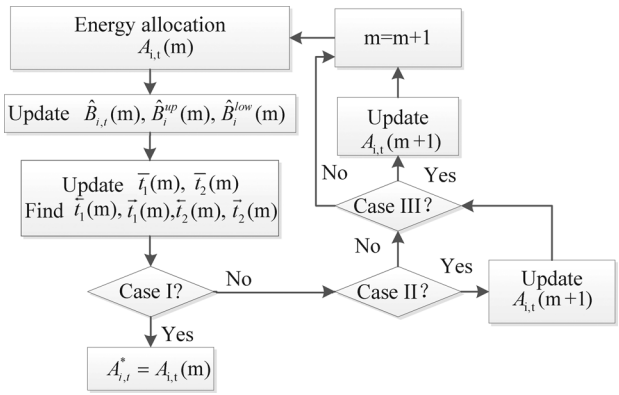

Fig. 2. The structure of BEAS.

Denote the slot by t' when $\hat{B}_i^{up}$ is reached and the slot by t'' when $\hat{B}_i^{low}$ is reached. If $\hat{B}_i^{up} > B_i^{\max}$, we set $\bar{t}_1 = t'$; otherwise, $\bar{t}_1 = 0$. Also, if $\hat{B}_i^{low} < 0$, we set $\bar{t}_2 = t''$; otherwise, $\bar{t}_2 = 0$. Hereby, $\bar{t}_1(\neq 0)$ and $\bar{t}_2(\neq 0)$ indicate the slots at which the virtual battery levels $\hat{B}_{i,t'}$ and $\hat{B}_{i,t''}$ reach $\hat{B}_i^{up}$ and $\hat{B}_i^{low}$, respectively. In order to make the energy allocation satisfy the second and fourth requirements, the total amount of energy allocation before $\bar{t}_1$ should be increased and the total amount of energy allocation before $\bar{t}_2$ should be decreased, respectively. Thus, we design a balanced energy allocation scheme to reduce $\hat{B}_i^{up}$ and increase $\hat{B}_i^{low}$ based on the values of $\bar{t}_1$ and $\bar{t}_2$. The detailed adjustment is given in the following.

Let m denote mth adjustment of energy allocation. Let $\hat{B}_i^{up}(m)$ and $\hat{B}_i^{low}(m)$ denote the upper and lower bound after $(m-1)$th adjustment, and $\bar{t}_1(m)$ and $\bar{t}_2(m)$ denote the corresponding slots, respectively. We set $\hat{t}(m) = \{0, T, \bar{t}_1(m), \bar{t}_2(m), \hat{t}(m-1)\}$, where $m = 1, 2, \ldots$, and $\hat{t}(0) = \varnothing$. Then, we define the following four parameters:

- $\overleftarrow{t}_1(m)$ is the largest slot in set $\hat{t}(m)$, which is smaller than $\bar{t}_1(m)$,
- $\overrightarrow{t}_1(m)$ is the smallest slot in set $\hat{t}(m)$, which is larger than $\bar{t}_1(m)$,
- $\overleftarrow{t}_2(m)$ is the largest slot in set $\hat{t}(m)$, which is smaller than $\bar{t}_2(m)$, and
- $\overrightarrow{t}_2(m)$ is the smallest slot in set $\hat{t}(m)$, which is larger than $\bar{t}_2(m)$.

For example, if $\hat{t}(m-1) = \{0, 3, 8, 15, 20, 24\}$, $\bar{t}_1(m) = 5$ and $\bar{t}_2 = 18$, then we have $\hat{t}(m) = \{0, 3, 5, 8, 15, 18, 20, 24\}$, $\overleftarrow{t}_1(m) = 3$, $\overrightarrow{t}_1(m) = 8$, $\overleftarrow{t}_2(m) = 15$ and $\overrightarrow{t}_2(m) = 20$. An illustration is shown in Fig. 1.

Based on the values of $\bar{t}_1(m)$ and $\bar{t}_2(m)$, the BEAS can be divided into three cases, which is elaborated in the following:

1) Case I: $\bar{t}_1(m) = \bar{t}_2(m) = 0$:

$$A_{i,t}^* = A_{i,t}(m). \tag{22}$$

2) Case II: $\bar{t}_1(m) \neq 0$:

$$A_{i,t}(m+1) = \begin{cases} A_{i,t}(m), & t \leq \overleftarrow{t}_1(m), \\ A_{i,t}(m) + \frac{\hat{B}_i^{up}(m) - B_i^{\max}}{\bar{t}_1(m) - \overleftarrow{t}_1(m)}, & \overleftarrow{t}_1(m) < t \leq \bar{t}_1(m), \\ A_{i,t}(m) - \frac{\hat{B}_i^{up}(m) - B_i^{\max}}{\overrightarrow{t}_1(m) - \bar{t}_1(m)}, & \bar{t}_1(m) < t \leq \overrightarrow{t}_1(m), \\ A_{i,t}(m), & \overrightarrow{t}_1(m) < t. \end{cases} \tag{23}$$

3) Case III: $\bar{t}_2(m) \neq 0$:

$$A_{i,t}(m+1) = \begin{cases} A_{i,t}(m), & t \leq \overleftarrow{t}_2(m), \\ A_{i,t}(m) + \frac{\hat{B}_i^{low}(m)}{\bar{t}_2(m) - \overleftarrow{t}_2(m)}, & \overleftarrow{t}_2(m) < t \leq \bar{t}_2(m), \\ A_{i,t}(m) - \frac{\hat{B}_i^{low}(m)}{\overrightarrow{t}_2(m) - \bar{t}_2(m)}, & \bar{t}_2(m) < t \leq \overrightarrow{t}_2(m), \\ A_{i,t}(m), & \overrightarrow{t}_2(m) < t. \end{cases} \tag{24}$$

At each iteration, $A_{i,t}$ will be updated according to (23) and (24) until $\bar{t}_1(m) = \bar{t}_2(m) = 0$. The structure of Algorithm 1 can be given by Fig. 2.

Different from a constant energy allocation scheme in existing algorithm, BEAS aims to dynamically allocate energy as smoothly as possible, while satisfying the aforementioned four requirements. It is easy to find that after mth adjustment, the battery level at slot t', $t' \in \hat{t}(m) \setminus \{0, T\})$, equals to $B_i^{\max}$ or 0. Furthermore, the battery level at slot t' will not change in the rest of adjustments. Thus, BEAS will converge to the optimal solution after at most T adjustments. We sketch BEAS in Algorithm 1 and have the following result about its performance.

Algorithm 1 Balanced Energy Allocation Scheme (BEAS)

repeat

for $t = 1, 2, \ldots, T$

• Each sensor updates the virtual battery level $\hat{B}_{i,t}(m)$ according to **(19)**.

• Each sensor updates the upper and lower bounds, $\hat{B}_i^{up}(m)$ and $\hat{B}_i^{low}(m)$, according to **(20)** and **(21)**, respectively. Meanwhile, the values of $\bar{t}_1(m)$ and $\bar{t}_2(m)$ are setted.

• Each sensor finds the values of $\overleftarrow{t}_1(m)$, $\overrightarrow{t}_1(m)$, $\overleftarrow{t}_2(m)$ and $\overrightarrow{t}_2(m)$, respectively.

end

• Each sensor updates its energy allocation $A_{i,t}(m+1)$ according to **(22)**–**(24)**.

• $m = m + 1$.

until $\bar{t}_1(m) = \bar{t}_2(m) = 0$

return $A_{i,t}^* = A_{i,t}(m)$

Theorem 1: Sensor i under BEAS will obtain a unique energy allocation, which satisfies the aforementioned four requirements.

Proof:

1) The initial energy allocation is $\pi_{i,t}$ and $\pi_{i,t} = \frac{1}{T}\sum_{t=1}^{T}\rho_{i,t}$. Hence, $\sum_{t=1}^{T}A_{i,t}(1) = \sum_{t=1}^{T}\rho_{i,t}$. We only need to prove that the total amount of energy allocation after the adjustment equals to the total amount of energy allocation before the adjustment.
   For Case I, since all the energy allocation are not changed, it satisfies the equality condition.
   For Case II, the BEAS only changes the energy allocation for slot t, $t \in [\overleftarrow{t_1}(m)+1, \overrightarrow{t_1}(m)]$. Thus, we only need to calculate the total mount of energy allocation for slot t, $t \in [\overleftarrow{t_1}(m)+1, \overrightarrow{t_1}(m)]$. As

$$\sum_{t=\overleftarrow{t_1}(m)+1}^{\bar{t}_1(m)} \frac{\hat{B}_i^{up}(m) - B_i^{\max}}{\bar{t}_1(m) - \overleftarrow{t_1}(m)} = \sum_{t=\bar{t}_1(m)+1}^{\overrightarrow{t_1}(m)} \frac{\hat{B}_i^{up}(m) - B_i^{\max}}{\overrightarrow{t_1}(m) - \bar{t}_1(m)}$$

   the total amount of energy allocation does not be changed by BEAS.
   For Case III, similar to Case II, we only need to calculate the total amount of energy allocation for slot t, $t \in [\overleftarrow{t_2}(m)+1, \overrightarrow{t_2}(m)]$. As

$$\sum_{t=\overleftarrow{t_2}(m)+1}^{\bar{t}_2(m)} \frac{\hat{B}_i^{low}(m)}{\bar{t}_2(m) - \overleftarrow{t_2}(m)} = \sum_{t=\bar{t}_2(m)+1}^{\overrightarrow{t_2}(m)} \frac{\hat{B}_i^{low}(m)}{\overrightarrow{t_2}(m) - \bar{t}_2(m)}$$

   the total amount of the energy allocation is not changed. Hence, we know that BEAS only changes the energy allocation in each slot, and does not change the total amount of energy allocation. Thus, we have

$$\sum_{t=1}^{T} A_{i,t}(m+1) = \sum_{t=1}^{T} A_{i,t}(m) = \cdots, = \sum_{t=1}^{T} A_{i,t}(1) = \sum_{t=1}^{T} \rho_{i,t}.$$

2) In BEAS, it is known that the necessary conditions for the convergence of BEAS is that the battery level should satisfies $\hat{B}_i^{up}(m) \le B_i^{\max}$ and $\hat{B}_i^{low}(m) \ge 0$ at the same time. Otherwise, the energy allocation will be updated until it satisfies these two necessary conditions. As $\hat{B}_i^{up}(m) \le B_i^{\max}$ means that the maximal battery level is not larger than $B_i^{\max}$, $o_{i,t}$ for each slot equals to zero. Thus, the total amount of the wasted energy is minimized. Since $\hat{B}_i^{low}(m) \ge 0$ means that the battery level for each slot always is no smaller than the energy allocation, each sensor never runs out of energy. Hence, the second and the fourth conditions are satisfied.

3) In the BEAS, if there exists a $\bar{t}_1(m)$ (or $\bar{t}_2(m)$), the first task for the sensor is to find the $\overleftarrow{t_1}(m)$ and $\overrightarrow{t_1}(m)$ (or $\overleftarrow{t_2}(m)$ and $\overrightarrow{t_2}(m)$), and the following task is to adjust the energy allocation. In order to prove that BEAS minimizes the variations of energy allocation, we need to prove that each adjustment of energy allocation minimizes the variations.

Assume that the $(m-1)$th adjustment minimizes the variations. We need to prove that the mth adjustment also minimizes the variations.

For Case I: since the energy allocation will not be changed, the variations will not be changed. Thus, the variations are minimized. Furthermore, it is easy to find that Case I indicates that the energy allocation converges to the optimal solution.

For Case II: since $\hat{B}_i^{up}(m)$ is larger than the $B_i^{\max}$, which means that the sensor needs to increase the energy allocation for the slots before $\bar{t}_1(m)$ to make battery level satisfy $\hat{B}_i^{up}(m+1) \le B_i^{\max}$. According to the definition of $\overleftarrow{t_1}(m)$, it can be found that there are two possible values for $\overleftarrow{t_1}(m)$: the first one is $\overleftarrow{t_1}(m) = \bar{t}_1(m')$ and the second one is $\overleftarrow{t_1}(m) = \bar{t}_2(m')$, where $m' \in \{1, 2, \ldots, m-1\}$. Now, we analyze the performance based on these two possible values, respectively.

$\hat{B}_{i,\overleftarrow{t_1}(m)}$

If $\overleftarrow{t_1}(m) = \bar{t}_1(m')$, the battery level $\hat{B}_{i,\overleftarrow{t_1}(m)}(m')$ is larger than $B_i^{\max}$ and $\hat{B}_{i,\overleftarrow{t_1}(m)}(m') \ge \hat{B}_{i,\bar{t}_1(m)}(m')$. Hence, we can obtain that $A_{i,\overleftarrow{t_1}(m)} \ge A_{i,t'}(m)$, where $t' \in (\overleftarrow{t_1}(m), \bar{t}_1(m)]$. This is because $\hat{B}_{i,\overleftarrow{t_1}(m)}(m')$ will be smaller than $\hat{B}_{i,\bar{t}_1(m)}(m')$ if $A_{i,t'}(m) \ge A_{i,\overleftarrow{t_1}(m)}$.

If $\overleftarrow{t_1}(m) = \bar{t}_2(m')$, the battery level $\hat{B}_{i,\overleftarrow{t_1}(m)}(m')$ is smaller than 0, and $\hat{B}_{i,\overleftarrow{t_1}(m)}(m') \le \hat{B}_{i,\bar{t}_1(m)}(m')$. After m'th adjustment, $\hat{B}_{i,\overleftarrow{t_1}(m)}(m')$ equals to 0, Hence, we cannot increase the energy allocation before $\overleftarrow{t_1}(m)$ and can only increase the energy allocation for the slots between $(\overleftarrow{t_1}(m), \bar{t}_1(m)]$, as, otherwise, the $\hat{B}_{i,\overleftarrow{t_1}(m)}(m')$ will be smaller than 0 again.

Hence, the sensor can only adjust the energy allocation between the $(\overleftarrow{t_1}(m), \bar{t}_1(m)]$ to decrease the $\hat{B}_i^{up}(m)$, as

$$\sum_{t=i,\overleftarrow{t_1}(m)}^{\bar{t}_1(m)} A_{i,t}(m+1) = \hat{B}_i^{up}(m) - B_i^{\max} + \sum_{t=\overleftarrow{t_1}(m)+1}^{\bar{t}_1(m)} A_{i,t}(m).$$

If we aim at minimizing $\sum_{t=\overleftarrow{t_1}(m)+1}^{\bar{t}_1(m)} (A_{i,t}(m+1) - \rho_{i,t})^2$, it is easy to find the optimal energy allocation, which is given by $A_{i,t}(m+1) = A_{i,t}(m) + \frac{\hat{B}_i^{up}(m) - B_i^{\max}}{\bar{t}_1(m) - \overleftarrow{t_1}(m)}$, $t \in (\overleftarrow{t_1}(m), \bar{t}_1(m)]$.

Similarly, there are two possible values for $\overrightarrow{t_1}(m)$: the first is $\overrightarrow{t_1}(m) = \bar{t}_1(m')$ and the second is $\overrightarrow{t_1}(m) = \bar{t}_2(m')$, where $m' \in \{1, 2, \ldots, m-1\}$. By a similar process, we can find that the sensor can only adjust the energy allocation between the $(\bar{t}_1(m), \overrightarrow{t_1}(m)]$ and the optimal energy allocation is given by $A_{i,t}(m+1) = A_{i,t}(m) - \frac{\hat{B}_i^{up}(m) - B_i^{\max}}{\overrightarrow{t_1}(m) - \bar{t}_1(m)}$, $t \in (\bar{t}_1(m), \overrightarrow{t_1}(m)]$.

For the Case III, since $\hat{B}_i^{low}(m)$ is smaller than 0, which means that the sensor needs to decrease the energy allocation for the slots before $\bar{t}_2(m)$ in order to make battery level $\hat{B}_i^{up}(m+1) \geq 0$. According to the definition of $\overleftarrow{t_2}(m)$, it can be found that there are two possible values for $\overleftarrow{t_2}(m)$: the first is $\overleftarrow{t_2}(m) = \bar{t}_1(m')$ and the second is $\overleftarrow{t_2}(m) = \bar{t}_2(m')$, where $m' \in 1, 2, \ldots, m-1$. We can analyze Case III in the same way as Case II. Thus we omit the detail. The optimal solution for Case III can be given as follows:

When $t \in (\overleftarrow{t_2}(m)+1, \bar{t}_2(m)]$,

$$A_{i,t}(m+1) = A_{i,t}(m) + \frac{\hat{B}_i^{low}(m)}{\bar{t}_2(m) - \overleftarrow{t_2}(m)} \tag{25}$$

and when $t \in (\bar{t}_2(m)+1, \overrightarrow{t_2}(m)]$,

$$A_{i,t}(m+1) = A_{i,t}(m) - \frac{\hat{B}_i^{low}(m)}{\overrightarrow{t_2}(m) - \bar{t}_2(m)}. \tag{26}$$

In general, we find that the mth adjustment is the optimal adjustment solution. Thus, we can conclude that each adjustment is the optimal adjustment solution for the energy allocation, which minimizes the variations in the energy allocation. ■

B. Distributed Sensing Rate and Routing Control

With the energy allocation $A_{i,t}^*$, calculated by BEAS, we proceed to design a distributed sensing rate and routing algorithm. Based on BEAS, the problem (12)–(17) can be rephrased as

$$objective \max_{x_{i,t}, f_{ij,t}, e_{ij,t}^{tr}} \sum_i \sum_t U(x_{i,t}) \tag{27}$$

$$s.t.\ f_{i,t}^{in} + x_{i,t} = f_{i,t}^{out}, \quad \forall i,t \tag{28}$$

$$A_{i,t}^* \geq P_{i,t}, \quad \forall i,t \tag{29}$$

$$e_{ij,t}^{tr} \geq E_{ij}, \quad \forall i,j \in \mathbb{O}(i), t. \tag{30}$$

In this optimization problem, the variables are sensing rates $\boldsymbol{x}$, flow rates $\boldsymbol{f}$ and transmit energy consumptions $\boldsymbol{e^{tr}}$. From the primal problem (27)–(30), it is easy to find that the primal problem is a convex optimization problem since the relationship between $e_{ij,t}^{tr}$ and $f_{ij,t}$ is independent. Thus, the primal problem can be solved by employing dual decomposition and sub-gradient method [30]. In such an approach, updating Lagrange multipliers of one sensor only relates to its neighbors' information and updating variables of one sensor only depends on its neighbors' Lagrange multipliers. However, this leads to the fact that the difference between two updates is very small. Thus, this approach has a very slow convergence rate in a large-scale sensor network. Note that there is an underlying relationship between $\boldsymbol{x}_t$ and $f_{ij,t}$, as $f_{ij,t}$ can be described as a function of $\boldsymbol{x}_t$. Thus, we transform this optimization problem into another one by employing variable substitution.

A summary of notation for matrix used in this paper is given in Table II.

Now, we introduce flow variables to describe the relationship between flow rates $\boldsymbol{f}$ and sensing rates $\boldsymbol{x}$. We define a diffluent matrix $\boldsymbol{h}$, where $h_{ij,t}$ represents the ratio of the total amount of sensory data that can be transmitted by sensor i using the logical link (i,j), to the total amount of sensory data that can be transmitted by sensor i at slot t, i.e.,

TABLE II
NOTATION DEFINITIONS OF MATRIX

Symbol	Definition
$\boldsymbol{I}$	$N \times N$ unit matrix
S	$N \times 1$ column vector, in which all the elements are 1
$(\cdot)^T$	The transpose of matrix $(\cdot)$
$(\cdot)_t$	The matrix $(\cdot)$ at slot t
$(\cdot)_{:,t}$	All the elements of the column vector $(\cdot)$ at slot t
$(\cdot)_{ij,t}$	The i-th row and j-th column element of matrix $(\cdot)$ at slot t
$(\cdot)_{i:,t}$	The i-th row elements of matrix $(\cdot)$ at slot t
$(\cdot)_{:i,t}$	The i-th column elements of matrix $(\cdot)$ at slot t
$(\cdot)_{(ij),t}$	All the elements of the matrix $(\cdot)$ are 0 except $(\cdot)_{ij,t}$ at slot t
$(\cdot)_{(i:),t}$	All the elements of the matrix $(\cdot)$ are 0 except $(\cdot)_{i:,t}$ at slot t
$(\cdot)_{(:i),t}$	All the elements of the matrix $(\cdot)$ are 0 except $(\cdot)_{:i,t}$ at slot t

$$h_{ij,t} = \begin{cases} \frac{f_{ij,t}}{f_{i,t}^{out}}, & \text{if } R_{ij} = 1, \\ 0, & \text{otherwise.} \end{cases} \tag{31}$$

In order to satisfy the flow conservation in (8), the diffluent matrix $\boldsymbol{h}$ needs to satisfy the following condition:

$$h_{i:,t} S = 1, \qquad \forall i,t \tag{32}$$

where S is a $N \times 1$ column vector, in which all the elements are 1. As the total number of sensors is N, the number of relays in the routing path of each sensor is at most N. Let

$$\boldsymbol{H}_t^{(1)} = \boldsymbol{h}_t,\ \boldsymbol{H}_t^{(2)} = \boldsymbol{H}_t^{(1)} + \boldsymbol{h}_t^2,$$
$$\boldsymbol{H}_t^{(3)} = \boldsymbol{H}_t^{(2)} + \boldsymbol{h}_t^3, \ldots, \boldsymbol{H}_t^{(n)} = \boldsymbol{H}_t^{(n-1)} + \boldsymbol{h}_t^n$$

where $\boldsymbol{h}_t^n = \boldsymbol{h}_t^{n-1}\boldsymbol{h}_t$ and n, $n \in [2, N]$, is the sequence number of transmission. Note that $\boldsymbol{H}_t^{(n)}$ is a function of $\boldsymbol{h}_t$, which is a constant in each slot.

Lemma 1: All the variables of flow rates can be expressed as functions of $\boldsymbol{x}$ and $\boldsymbol{h}$, i.e.,

$$f_{ij,t} = x_{:,t}^T \boldsymbol{H}_{(ij),t}^{(N)} S \tag{33}$$

$$f_{i,t}^{in} = x_{:,t}^T H_{:i,t}^{(N)} \tag{34}$$

$$f_{i,t}^{out} = x_{:,t}^T \hat{\boldsymbol{H}}_t^{(N)} \boldsymbol{H}_{(i:),t}^{(1)} S \tag{35}$$

where $\hat{\boldsymbol{H}}_t^{(N)} = (\boldsymbol{I} + \boldsymbol{H}_t^{(N-1)})$ and $\boldsymbol{I}$ is a $N \times N$ unit matrix.

Proof: According to the definition of $\boldsymbol{H}$ and the properties of matrix multiplication, $\boldsymbol{H}_t^{(n)}$ and $\boldsymbol{H}_{(ij),t}^{(n)}$ can be given by

$$\boldsymbol{H}_t^{(n)} = \boldsymbol{h}_t + \boldsymbol{h}_t^2 + \boldsymbol{h}_t^3 + \cdots + \boldsymbol{h}_t^n \tag{36}$$

$$\boldsymbol{H}_{(ij),t}^{(n)} = (\boldsymbol{I} + \boldsymbol{h}_t + \boldsymbol{h}_t^2 + \boldsymbol{h}_t^3 + \cdots + \boldsymbol{h}_t^{n-1}) h_{(ij),t}$$
$$= \hat{\boldsymbol{H}}_t^{(n)} \boldsymbol{h}_{(ij),t} \tag{37}$$

where $\hat{\boldsymbol{H}}_t^{(n)} = (\boldsymbol{I} + \boldsymbol{H}_t^{(n-1)})$ and $n \in [2, N]$. Since one sensor only serves as relay node for the other sensors, which are farther away from sink node, all the flows are unidirectional and there is no cycle routing in the network topology. Let $f_{ij,t}^{(n)}$ denote the total amount of sensory data that will be transmitted by sensor i after $n-1$ times relays from the source sensors using the logical link (i, j). We have

$$\begin{aligned} f_{ij,t}^{(1)} &= x_{:,t}^T \boldsymbol{h}_{(ij),t} S \\ f_{ij,t}^{(2)} &= x_{:,t}^T \boldsymbol{h}_t \boldsymbol{h}_{(ij),t} S \\ &\cdots \\ f_{ij,t}^{(N)} &= x_{:,t}^T \boldsymbol{h}_t^{N-1} \boldsymbol{h}_{(ij),t} S. \end{aligned}$$

It can be found that $f_{ij,t}^{(1)}$ denotes the total amount of data (sensed by sensor i) sent out by sensor i using link (i, j), $f_{ij,t}^{(2)}$ denotes the total amount of data (received by sensor i from its front sensors, which are the source sensors, after 1 time relay) sent out by sensor i using link (i, j). Similarly, $f_{ij,t}^{(n)}$ denotes the total amount of data (received by sensor i after $n-1$ times relays from the source sensor) sent out by sensor i using link (i, j). Thus, the total amount of sensory data that can be transmitted by sensor i using the logical link (i, j) is

$$\begin{aligned} f_{ij,t} &= f_{ij,t}^{(1)} + f_{ij,t}^{(2)} + f_{ij,t}^{(3)} + \cdots + f_{ij,t}^{(N)} \\ &= x_{:,t}^T (\boldsymbol{I} + \boldsymbol{h}_t + \boldsymbol{h}_t^2 + \cdots + \boldsymbol{h}_t^{N-1}) \boldsymbol{h}_{(ij),t} S \\ &= x_{:,t}^T \hat{\boldsymbol{H}}_{(ij),t}^{(N)} S. \end{aligned}$$

Similarly, we have

$$\begin{aligned} f_{i,t}^{in} &= \sum_{k \in \mathbb{I}(i)} x_{:,t}^T (\boldsymbol{I} + \boldsymbol{h}_t + \boldsymbol{h}_t^2 + \cdots + \boldsymbol{h}_t^{N-1}) \boldsymbol{h}_{(ki),t} S \\ &= x_{:,t}^T (\boldsymbol{I} + \boldsymbol{h}_t + \boldsymbol{h}_t^2 + \cdots + \boldsymbol{h}_t^{N-1}) h_{:i,t} \\ &= x_{:,t}^T H_{:i,t}^{(N)}, \\ f_{i,t}^{out} &= \sum_{j \in \mathbb{O}(i)} x_{:,t}^T (\boldsymbol{I} + \boldsymbol{h}_t + \boldsymbol{h}_t^2 + \cdots + \boldsymbol{h}_t^{N-1}) \boldsymbol{h}_{(ij),t} S \\ &= x_{:,t}^T (\boldsymbol{I} + \boldsymbol{h}_t + \boldsymbol{h}_t^2 + \cdots + \boldsymbol{h}_t^{N-1}) \boldsymbol{h}_{(i:),t} S \\ &= x_{:,t}^T \hat{\boldsymbol{H}}_t^{(N)} \boldsymbol{H}_{(i:),t}^{(1)} S. \end{aligned}$$

■

Now, (28) and (29) can be rewritten as follows:

$$x_{:,t}^T H_{:i,t}^{(N)} + x_{i,t} = x_{:,t}^T \hat{\boldsymbol{H}}_t^{(N)} \boldsymbol{H}_{(i:),t}^{(1)} S, \tag{38}$$

$$e_i^{re} x_{:,t}^T H_{:i,t}^{(N)} + e_i^{sn} x_{i,t} + x_{:,t}^T \hat{\boldsymbol{H}}_t^{(N)} \boldsymbol{Q}_{(i:),t} S \le A_{i,t}, \tag{39}$$

where

$$\boldsymbol{Q}_{ij,t} = \begin{cases} H_{ij,t}^{(1)} e_{ij,t}^{tr}, & \text{if } H_{ij,t}^{(1)} \neq 0 \\ 0, & \text{otherwise.} \end{cases} \tag{40}$$

The optimization problem (27)–(30) can be rephrased as

$$Objective \quad \max_{x_{i,t}, h_{ij,t}, e_{ij,t}^{tr}} \sum_i \sum_t U(x_{i,t}) \tag{41}$$

$$s.t. \quad e_{ij,t}^{tr} \ge E_{ij}, \quad \forall i, j \in \mathbb{O}(i), t \tag{42}$$

$$h_{i:,t} S = 1, \quad \forall i, t \tag{43}$$

$$x_{:,t}^T H_{:i,t}^{(N)} + x_{i,t} = x_{:,t}^T \hat{\boldsymbol{H}}_t^{(N)} \boldsymbol{H}_{(i:),t}^{(1)} S, \quad \forall i, t \tag{44}$$

$$e_i^{re} x_{:,t}^T H_{:i,t}^{(N)} + e_i^{sn} x_{i,t} + x_{:,t}^T \hat{\boldsymbol{H}}_t^{(N)} \boldsymbol{Q}_{(i:),t} S \le A_{i,t}, \quad \forall i, t. \tag{45}$$

By employing dual decomposition and sub-gradient methods, we design a DSR2C algorithm to solve the optimization problem (41)–(45).

Through relaxing (42) with Lagrange multipliers $\boldsymbol{\tau}$, (43) with Lagrange multipliers $\boldsymbol{\gamma}$, (44) with Lagrange multipliers $\boldsymbol{\eta}$ and (45) with Lagrange multipliers $\boldsymbol{\theta}$, respectively, the dual problem is given as follows:

$$\begin{aligned} D(\boldsymbol{\tau}, \boldsymbol{\gamma}, \boldsymbol{\eta}, \boldsymbol{\theta}) = \max_{x_{i,t}, h_{ij,t}, e_{ij,t}^{tr}} \sum_i \sum_t \Big\{ & U(x_{i,t}) + \gamma_{i,t}(1 - h_{i:,t} S) \\ & + \eta_{i,t}(x_{:,t}^T \hat{\boldsymbol{H}}_t^{(N)} \boldsymbol{H}_{(i:),t}^{(1)} S - x_{:,t}^T H_{:i,t}^{(N)} - x_{i,t}) \\ & + \theta_{i,t}(A_{i,t} - e_i^{re} x_{:,t}^T H_{:i,t}^{(N)} - e_i^{sn} x_{i,t} \\ & - x_{:,t}^T \hat{\boldsymbol{H}}_t^{(N)} \boldsymbol{Q}_{(i:),t} S) + \sum_{j \in \mathbb{O}(i)} \tau_{ij,t}(e_{ij,t}^{tr} - E_{ij}) \Big\}. \end{aligned}$$

The dual problem of (41)–(45) is

$$\min_{\tau_{ij,t}, \gamma_{i,t}, \eta_{i,t}, \theta_{i,t}} D(\boldsymbol{\tau}, \boldsymbol{\eta}, \boldsymbol{\theta}, \boldsymbol{\gamma}). \tag{46}$$

This dual problem can be decomposed in each slot t, i.e.,

$$\begin{aligned} & D_t(\boldsymbol{\tau}_t, \boldsymbol{\eta}_t, \boldsymbol{\theta}_t, \boldsymbol{\gamma}_t) \\ &= \max_{x_{i,t}, h_{ij,t}, e_{ij,t}^{tr}} \sum_i \Big\{ U(x_{i,t}) + \gamma_{i,t}(1 - h_{i:,t} S) \\ & \quad + \eta_{i,t}(x_{:,t}^T \hat{\boldsymbol{H}}_t^{(N)} \boldsymbol{H}_{(i:),t}^{(1)} S - x_{:,t}^T H_{:i,t}^{(N)} - x_{i,t}) \\ & \quad + \theta_{i,t}(A_{i,t} - e_i^{re} x_{:,t}^T H_{:i,t}^{(N)} - e_i^{sn} x_{i,t} \\ & \quad - x_{:,t}^T \hat{\boldsymbol{H}}_t^{(N)} \boldsymbol{Q}_{(i:),t} S) + \sum_{j \in \mathbb{O}(i)} \tau_{ij,t}(e_{ij,t}^{tr} - E_{ij}) \Big\}. \end{aligned} \tag{47}$$

Let $\boldsymbol{\tau}_t = (\tau_{ij,t}, i, j = 1, 2, \ldots, N)$, $\boldsymbol{\gamma}_t = (\gamma_{i,t}, i = 1, 2, \ldots, N)$, $\boldsymbol{\eta}_t = (\eta_{i,t}, i = 1, 2, \ldots, N)$ and $\boldsymbol{\theta}_t = (\theta_{i,t}, i = 1, 2, \ldots, N)$. For simplicity, we use e^{sn} and e^{re} denote the average energy cost for sensing and receiving one unit data. The dual problem $D_t(\boldsymbol{\tau}_t, \boldsymbol{\eta}_t, \boldsymbol{\theta}_t, \boldsymbol{\gamma}_t)$ can be rephrased as follows:

$$\begin{aligned} & D_t(\boldsymbol{\tau}_t, \boldsymbol{\eta}_t, \boldsymbol{\theta}_t, \boldsymbol{\gamma}_t) \\ &= \max_{x_{i,t}, h_{ij,t}, e_{ij,t}^{tr}} \sum_i \{ U(x_{i,t}) + \boldsymbol{\gamma}_t(S - h_t S) \\ & \quad + \eta_{i,t} x_{:,t}^T \hat{\boldsymbol{H}}_t^{(N)} \boldsymbol{H}_{(i:),t}^{(1)} S - \theta_{i,t} x_{:,t}^T \hat{\boldsymbol{H}}_t^{(N)} \boldsymbol{Q}_{(i:),t} S \} \\ & \quad + A_{:,t} \boldsymbol{\theta}_t^T - x_{:,t}^T \boldsymbol{H}_l^{(N)} (\boldsymbol{\eta}_t^T + e^{re} \boldsymbol{\theta}_t^T) \\ & \quad - x_{:,t} (\boldsymbol{\eta}_t^T + e^{sn} \boldsymbol{\theta}_t^T) + \sum_i \sum_{j \in \mathbb{O}(i)} \tau_{ij,t}(e_{ij,t}^{tr} - E_{ij}). \end{aligned} \tag{48}$$

Due to the convexity and differentiability of (41), the sub-gradient method can be adopted to update the Lagrange multipliers $\tau_{ij,t}$, $\gamma_{i,t}$, $\eta_{i,t}$ and $\theta_{i,t}$ iteratively at each sensor according to

$$\tau_{ij,t}(m+1) = [\tau_{ij,t}(m) - \epsilon(e_{ij}^{tr} - E_{ij})]^+ \tag{49}$$

$$\gamma_{i,t}(m+1) = \gamma_{i,t}(m) - \epsilon(1 - h_{i:,t}S) \tag{50}$$

$$\begin{aligned}\eta_{i,t}(m+1) = \eta_{i,t}(m) &- \epsilon(x_{:,t}^T \hat{\boldsymbol{H}}_t^{(N)} \boldsymbol{H}_{(i:),t}^{(1)} S \\ &- x_{:,t}^T H_{:i,t}^{(N)} - x_{i,t})\end{aligned} \tag{51}$$

$$\begin{aligned}\theta_{i,t}(m+1) = [\theta_{i,t}(m) &- \epsilon(A_{i,t} - e^{re} x_{:,t}^T H_{:i,t}^{(N)} \\ &- e^{sn} x_{i,t} - x_{:,t}^T (\hat{\boldsymbol{H}}_t^{(N)}) \boldsymbol{Q}_{(i:),t} S)]^+\end{aligned} \tag{52}$$

where m is the iteration number, ϵ is step size, satisfying $\epsilon > 0$, and $[\cdot]^+ = \max(0, \cdot)$.

Since $U(x_{i,t})$ is a strictly concave function of $x_{i,t}$ and all the constraints are continuously differentiable for $x_{i,t}$, $h_{ij,t}$ and $e_{ij,t}^{tr}$, respectively, we have that $D_t(\tau_t, \eta_t, \theta_t, \gamma_t)$ is continuously differentiable for $x_{i,t}$, $h_{ij,t}$ and $e_{ij,t}^{tr}$, respectively. The derivatives of $D_t(\tau_t, \eta_t, \theta_t, \gamma_t)$ with respect to $x_{i,t}$, $h_{ij,t}$ and $e_{ij,t}^{tr}$ can be calculated by

$$\frac{\partial D_t(\boldsymbol{\tau}_t, \boldsymbol{\eta}_t, \boldsymbol{\theta}_t, \boldsymbol{\gamma}_t)}{\partial x_{i,t}} = U'(x_{i,t}) + \Phi(x_{i,t}) \tag{53}$$

$$\frac{\partial D_t(\boldsymbol{\tau}_t, \boldsymbol{\eta}_t, \boldsymbol{\theta}_t, \boldsymbol{\gamma}_t)}{\partial h_{ij,t}} = \Phi_1(h_{ij,t}) \tag{54}$$

$$\frac{\partial D_t(\boldsymbol{\tau}_t, \boldsymbol{\eta}_t, \boldsymbol{\theta}_t, \boldsymbol{\gamma}_t)}{\partial e_{ij,t}^{tr}} = \Phi_2(e_{ij,t}^{tr}) \tag{55}$$

where

$$\begin{aligned}\Phi(x_{i,t}) = \sum_k \{&\eta_{k,t} S_{(i)}^T \hat{\boldsymbol{H}}_t^{(N)} \boldsymbol{H}_{(k:),t}^{(1)} S \\ &- \theta_{k,t} S_{(i)}^T (\hat{\boldsymbol{H}}_t^{(N)}) \boldsymbol{Q}_{(k:),t} S\} \\ &- S_{(i)}^T \boldsymbol{H}_t^{(N)} (\eta_t^T + e^{re} \theta_t^T) - S_{(i)}^T (\eta_t^T + e^{sn} \theta_t^T)\end{aligned} \tag{56}$$

$$\begin{aligned}\Phi_1(h_{ij,t}) = &- \gamma_{i,t} - x_{:,t}^T \frac{\partial \boldsymbol{H}_t^{(N)}}{\partial h_{ij,t}} (\eta_t^T + e^{re} \theta_t^T) \\ &+ \eta_{i,t} x_{:,t}^T \hat{\boldsymbol{H}}_t^{(N)} \frac{\partial \boldsymbol{H}_{(i:),t}^{(1)}}{\partial h_{ij,t}} S - \theta_{i,t} x_{:,t}^T \hat{\boldsymbol{H}}_t^{(N)} \frac{\partial \boldsymbol{Q}_{(i:),t}}{\partial h_{ij,t}} S \\ &+ \sum_{k,k \neq i} \left\{ \eta_{k,t} x_{:,t}^T \frac{\partial \hat{\boldsymbol{H}}_t^{(N)}}{\partial h_{ij,t}} \boldsymbol{H}_{(k:),t}^{(1)} S \right. \\ &\left. - \theta_{k,t} x_{:,t}^T \frac{\partial \hat{\boldsymbol{H}}_t^{(N)}}{\partial h_{ij,t}} \boldsymbol{Q}_{(k:),t} S \right\}\end{aligned} \tag{57}$$

$$\Phi_2(e_{ij,t}^{tr}) = \tau_{ij,t} - \theta_{i,t} x_{:,t}^T \hat{H}_t^{(N)} h_{(i:),t} S. \tag{58}$$

According to the properties of matrix derivation, we have

$$\frac{\partial \boldsymbol{H}_{(i:),t}^{(1)}}{\partial h_{ij,t}} = \begin{cases} 1, & \text{if } k = i \text{ and } l = j, \\ 0, & \text{otherwise,} \end{cases} \tag{59}$$

$$\frac{\partial \boldsymbol{Q}_{(i:),t}}{\partial h_{ij,t}} = \begin{cases} e_{kl,t}^{tr}, & \text{if } k = i \text{ and } l = j, \\ 0, & \text{otherwise,} \end{cases} \tag{60}$$

$$\frac{\partial \hat{\boldsymbol{H}}_t^{(N)}}{\partial h_{ij,t}} = \frac{\partial \boldsymbol{H}_t^{(N-1)}}{\partial h_{ij,t}} \tag{61}$$

$$\begin{aligned}\frac{\partial \boldsymbol{H}_t^{(n)}}{\partial h_{ij,t}} &= \frac{\partial \boldsymbol{h}_t^1}{\partial h_{ij,t}} + \frac{\partial \boldsymbol{h}_t^2}{\partial h_{ij,t}} + \cdots + \frac{\partial \boldsymbol{h}_t^n}{\partial h_{ij,t}} \\ &= \frac{\partial \boldsymbol{h}_t^1}{\partial h_{ij,t}} + \frac{\partial \boldsymbol{h}_t}{\partial h_{ij,t}} \boldsymbol{h}_t + \boldsymbol{h}_t \frac{\partial \boldsymbol{h}_t}{\partial h_{ij,t}} + \cdots + \frac{\partial \boldsymbol{h}_t}{\partial h_{ij,t}} \boldsymbol{h}_t^{n-1} \\ &\quad + \boldsymbol{h}_t \frac{\partial \boldsymbol{h}_t}{\partial h_{ij,t}} \boldsymbol{h}_t^{n-2} + \cdots + \boldsymbol{h}_t^{n-1} \frac{\partial \boldsymbol{h}_t}{\partial h_{ij,t}}\end{aligned} \tag{62}$$

where $n \in [2, N]$, k denotes a sensor excluding sink node, and l denotes a sensor or sink node. Note that each sensor does not need to know all the elements of $\boldsymbol{h}$, since only the values related to its data transmission can affect the values of $\Phi_1(h_{ij,t})$.

By using the KKT optimality, the extremal points for the $x_{i,t}$, $h_{ij,t}$ and $e_{ij,t}^{tr}$ can be obtained as

$$\begin{aligned}x_{i,t}^* &= \max_{x_{i,t}, h_{ij,t}} D_t(\eta_t, \theta_t, \gamma_t) \\ &= [U'^{-1}(-\Phi(x_{i,t}))]_0^{x_i^{\max}}\end{aligned} \tag{63}$$

$$h_{ij,t}(m+1) = \begin{cases} [h_{ij,t}(m) + \epsilon \Phi_1(h_{ij,t})]^+, & \text{if } R_{ij} = 1, \\ 0, & \text{otherwise,} \end{cases} \tag{64}$$

$$e_{ij,t}^{tr}(m+1) = \begin{cases} [e_{ij,t}^{tr}(m) + \epsilon \Phi_2(e_{ij,t}^{tr})]^+, & \text{if } R_{ij} = 1, \\ 0, & \text{otherwise.} \end{cases} \tag{65}$$

We sketch DSR2C in Algorithm 2 and have the following results on the performance of DSR2C algorithm.

Theorem 2: For a sufficiently small positive constant ϵ and optimal energy allocation $\boldsymbol{A}^*$, the DSR2C algorithm will converge to optimal solution.

Proof: Since the primal problem is a convex optimization problem, the global optimal solution can be obtained by employing dual decomposition and sub-gradient method [30]. After variable substitution, the primal problem can be rephrased as another transformed problem. By using the gradient method, $x_{i,t}$, $h_{ij,t}$ and $e_{ij,t}^{tr}$ for the transformed problem will converge to their extremal points, respectively. Thus, we only need to prove that the extremal points are the global optimal points.

Algorithm 2 DSR2C

Initialization ($\boldsymbol{A}^*$, $\boldsymbol{E}$)

repeat

for $i = 1, 2, \ldots, N$

• Each sensor locally updates the Lagrange multipliers $\tau_{ij,t}$, $\gamma_{i,t}$, $\eta_{i,t}$ and $\theta_{i,t}$ using **(49)**, **(50)**, **(51)** and **(52)**, respectively.

• Each sensor sends its $h_{i:,t}$, $e_{i:,t}^{tr}$ and Lagrange multipliers to sensor j, $j \in \mathbb{I}(i)$, meanwhile collecting and forwarding all the information from sensor j, $j \in \mathbb{O}(i)$.

• Each sensor calculates its sensing rate $x_{i,t}$, diffluent matrix $h_{i:,t}$ and transmits energy consumption $e_{i:,t}^{tr}$ using **(63)**, **(64)** and **(65)**, respectively.

end

until $\boldsymbol{x}_t(m+1) = \boldsymbol{x}_t(m)$, $\boldsymbol{h}_t(m+1) = \boldsymbol{h}_t(m)$ and $\boldsymbol{e}_t^{tr}(m+1) = \boldsymbol{e}_t^{tr}(m)$

return $\boldsymbol{x}_t(m)$, $\boldsymbol{h}_t(m)$ and $\boldsymbol{e}_t^{tr}(m)$.

Let D'_t be the Lagrangian function of the primal problem (27)–(30) and D_t be the Lagrangian function of the transformed problem (41)–(45), respectively.[2] Thus, we have

$$\frac{\partial D_t}{\partial x_{i,t}} = \frac{\partial D'_t}{\partial x_{i,t}} + \sum_k \sum_l \frac{\partial D'_t}{\partial f_{kl,t}} \frac{\partial f_{kl,t}}{\partial x_{i,t}} \tag{66}$$

$$\frac{\partial D_t}{\partial h_{ij,t}} = \sum_k \sum_l \frac{\partial D'_t}{\partial f_{kl,t}} \frac{\partial f_{kl,t}}{\partial h_{ij,t}} \tag{67}$$

$$\frac{\partial D_t}{\partial e^{tr}_{ij,t}} = \frac{\partial D'_t}{\partial e^{tr}_{ij,t}}. \tag{68}$$

According to the properties of matrix derivation given by (59)–(62), $\frac{\partial f_{kl,t}}{\partial h_{ij,t}} \geq 0, \forall k, l$, and $\frac{\partial f_{ij,t}}{\partial h_{ij,t}} > 0$ always holds. If $\frac{\partial f_{kl,t}}{\partial h_{ij,t}} = 0$, the data transmitted through link (k, l) does not go through link (i, j). If the constraint (44) is satisfied, constraint (43) will always holds. Thus, we omit it in (67). Using the KKT optimality conditions, the necessary condition associated with $h_{ij,t}$ is that $\sum_k \sum_l \frac{\partial D'_t}{\partial f_{kl,t}} \frac{\partial f_{kl,t}}{\partial h_{ij,t}} = 0$. We can prove that $\frac{\partial D'_t}{\partial f_{kl,t}} = 0, \forall k, l$, holds. Let s denote the sink node and (i, s) denote the link through which sensor i transmits data to sink node directly. Since only flow $f_{is,t}$ is transmitted through the link (i, s), $\sum_k \sum_l \frac{\partial D'_t}{\partial f_{kl,t}} \frac{\partial f_{kl,t}}{\partial h_{is,t}} = \frac{\partial D'_t}{\partial f_{is,t}} \frac{\partial f_{is,t}}{\partial h_{is,t}} = 0$ holds. Due to $\frac{\partial f_{is,t}}{\partial h_{is,t}} > 0$, we have $\frac{\partial D'_t}{\partial f_{is,t}} = 0$. Let k be a sensor who can transmit data to sensor i through link (k, i). According to the definition of $\boldsymbol{h}_t$, $\sum_k \sum_l \frac{\partial D'_t}{\partial f_{kl,t}} \frac{\partial f_{kl,t}}{\partial h_{ki,t}} = \frac{\partial D'_t}{\partial f_{ki,t}} \frac{\partial f_{ki,t}}{\partial h_{ki,t}} + \frac{\partial D'_t}{\partial f_{is,t}} \frac{\partial f_{is,t}}{\partial h_{ki,t}} = 0$ holds. Since $\frac{\partial D'_t}{\partial f_{is,t}} = 0$ and $\frac{\partial f_{ki,t}}{\partial h_{ki,t}} > 0$, $\frac{\partial D'_t}{\partial f_{ki,t}} = 0$ holds. Similarly, we can show that $\frac{\partial D'_t}{\partial f_{kl,t}} = 0, \forall k, l$, holds. Hence, the necessary condition associated with optimal $h_{ij,t}$ is the same as that associated with optimal $f_{ij,t}$.

Due to $\frac{\partial D'_t}{\partial f_{kl,t}} = 0, \forall k, l$, we have $\frac{\partial D_t}{\partial x_{i,t}} = \frac{\partial D'_t}{\partial x_{i,t}}$. Thus, the necessary conditions associated with optimal $x_{i,t}$, $h_{ij,t}$ and $e^{tr}_{ij,t}$ in transformed problem (41)–(45) are the same as these in primal problem (27)–(30). Since the primal problem is a convex problem, these necessary conditions correspond to the global optimal solution of the primal problem. This means that our proposed algorithm finds the global optimal solution of the primal problem. ■

If all sensors can transmit data to sink node directly, such as $e^{tr}_{ij} \in [0, \infty)$, the following properties for the optimal solution can be obtained by DSR2C:

Lemma 2: The total amount of utility $\sum U(x^*_{i,t})$ will increase as energy allocation of any sensor increases.

Proof: Please see the proof in supplementary document. ■

Lemma 3: In order to maximize network utility, all the sensors will consume all the allocated energy.

Proof: Please see the proof in supplementary document. ■

Lemma 4: For the optimal solution, the transmit energy consumption e^{tr}_{ij} should equal to the minimal transmit energy consumption E_{ij}, which is given by (5).

Proof: Please see the proof in supplementary document. ■

[2]For simplicity, we do not present the variables for D'_t and D_t.

According to Lemma 3 and 4, the optimization problem can be rewritten as

$$objective \quad \max_{x_{i,t}, h_{ij,t}} \quad \sum_i U(x_{i,t}) \tag{69}$$

$$s.t. \quad x^T_{:,t} H^{(N)}_{:i,t} + x_{i,t} = x^T_{:,t} \hat{\boldsymbol{H}}^{(N)}_t \boldsymbol{H}^{(1)}_{(i:),t} S, \tag{70}$$

$$e^{re}_i x^T_{:,t} H^{(N)}_{:i,t} + e^{sn}_i x_{i,t} + x^T_{:,t} \hat{\boldsymbol{H}}^{(N)}_t \boldsymbol{Q}_{(i:),t} S = A_{i,t}. \tag{71}$$

Since the transmit energy consumptions for all sensors are given, variables in this optimization problem are $\boldsymbol{x}_t$ and $\boldsymbol{h}_t$. Also, we can derive that this problem has optimal solution, since there exists at leat one available solution, i.e., all the sensors transmit their data to sink node directly. Thus, there exists an optimal matrix $\boldsymbol{M}_t$[3] to obtain the optimal solution, while satisfying the aforementioned constraints, i.e., $x^T_{:,t} * \boldsymbol{M}_t = \boldsymbol{A}^T_t$. Let $x_{i,t}$ be $((\boldsymbol{M}^{-1}_t)_{:i})^T \boldsymbol{A}_t$ and the total utility can be given by $\sum_i U(((\boldsymbol{M}^{-1}_t)_{:i})^T \boldsymbol{A}_t)$.

Theorem 3: For the different energy allocation $\boldsymbol{A}_t$ and $\boldsymbol{A}'_t$, we have the following property for total amount of utility:

$$\sum_i U(((\boldsymbol{M}'^{-1}_t)_{:i})^T \boldsymbol{A}'_t) - \sum_i U(((\boldsymbol{M}^{-1}_t)_{:i})^T \boldsymbol{A}_t) \leq \sum_i U(((\boldsymbol{M}''^{-1}_t)_{:i})^T (\boldsymbol{A}'_t - \boldsymbol{A}_t)) \tag{72}$$

where $\boldsymbol{A}'_t > \boldsymbol{A}_t$ means that at least one of the sensor's energy consumption $A'_{i,t}$ is larger than $A_{i,t}$ and other sensors' energy consumption $A'_{j,t}$, $j \neq i$, is not smaller than $A_{j,t}$, $\boldsymbol{A}'_t - \boldsymbol{A}_t = \{A'_{i,t} - A_{i,t}, i = 1, 2, \ldots, N\}$, M_t, M'_t and M''_t denote the optimal matrix for the energy allocation $\boldsymbol{A}_t, \boldsymbol{A}'_t$ and $\boldsymbol{A}'_t - \boldsymbol{A}_t$, respectively.

Proof: Please see the proof in supplementary document. ■

Theorem 4: The total amount of utility is a concave function of energy allocation $\boldsymbol{A}_t$.

Proof: Assume that there are three different energy allocations $\boldsymbol{A}'_t$, $\boldsymbol{A}_t$ and $\boldsymbol{A}''_t$, where $\boldsymbol{A}'_t > \boldsymbol{A}_t > \boldsymbol{A}''_t$, $2\boldsymbol{A}_t > \boldsymbol{A}'_t$ and $2\boldsymbol{A}_t = \boldsymbol{A}'_t + \boldsymbol{A}''_t$, $\boldsymbol{M}_t, \boldsymbol{M}'_t$ and $\boldsymbol{M}''_t$ denote the optimal matrix for the energy allocation $\boldsymbol{A}_t, \boldsymbol{A}'_t$ and $\boldsymbol{A}''_t$, respectively. For the optimal solution, it is known that $\boldsymbol{A}'_t = \boldsymbol{P}'_t$, $\boldsymbol{A}_t = \boldsymbol{P}_t$ and $\boldsymbol{A}''_t = \boldsymbol{P}''_t$. According to the Theorem 3, we have

$$\sum_i U(((\boldsymbol{M}'^{-1}_t)_{:i})^T \boldsymbol{A}'_t) > \sum_i U(((\boldsymbol{M}^{-1}_t)_{:i})^T \boldsymbol{A}_t) > \sum_i U(((\boldsymbol{M}''^{-1}_t)_{:i})^T \boldsymbol{A}''_t).$$

Let $\boldsymbol{x}'_{i,t} = ((M'^{-1}_t)_{:i})^T \boldsymbol{A}'_t$, $\boldsymbol{x}_{i,t} = ((\boldsymbol{M}^{-1}_t)_{:i})^T \boldsymbol{A}_t$ and $\boldsymbol{x}''_{i,t} = ((\boldsymbol{M}''^{-1}_t)_{:i})^T \boldsymbol{A}''_t$. Thus, we have $\boldsymbol{x}_t \geq \frac{\boldsymbol{x}'_t + \boldsymbol{x}''_t}{2}$ since sensors can send out a mount of $\frac{\boldsymbol{x}'_t}{2}$ data using matrix $\boldsymbol{M}_t$ and a amount of $\frac{\boldsymbol{x}''_t}{2}$ data using matrix $\boldsymbol{M}''_t$, and the total amount of energy cost is $\boldsymbol{A}_t = \frac{\boldsymbol{A}'_t + \boldsymbol{A}''_t}{2}$. Due to the optimal matrix $\boldsymbol{M}_t$, the total amount

[3]Here, $\boldsymbol{M}_t$ can be viewed as a function of the diffluent matrix $\boldsymbol{h}_t$, but more complicate than $\boldsymbol{h}_t$. Furthermore, the matrix $\boldsymbol{M}_t$ is full rank since matrix $\boldsymbol{M}_t$ can be converted into an upper triangular matrix and the determinant of the matrix only relates to the e^{sn}_i.

of utility will satisfy $\sum_i U(\boldsymbol{x}_{i,t}) \geq \sum_i U\left(\frac{\boldsymbol{x}'_{i,t}+\boldsymbol{x}''_{i,t}}{2}\right)$. Since the objective function is an increasing and concave function, we have

$$\sum_i U(\boldsymbol{x}'_{i,t}) + \sum_i U(\boldsymbol{x}''_{i,t}) < 2\sum_i U(\frac{\boldsymbol{x}'_{i,t}+\boldsymbol{x}''_{i,t}}{2}) \leq 2\sum_i U(\boldsymbol{x}_{i,t}), \quad (73)$$

which shows that the total amount of the utility is a concave function of energy allocation $\boldsymbol{A}_t$. ■

Since the total amount of utility is a concave function of energy allocation for any $A_{i,t}$ and the total harvested energy for each sensor is given, the optimal energy allocation needs to minimize the variation of energy allocation. Thus, in this paper, we take $\sum_{t=1}^{T}(A_{i,t}-\rho_{i,t})^2$ as the objective function and prove that the variation of energy allocation is minimized in Theorem 1.

C. Improved BEAS

Computing the optimal data sensing and data transmission strategies more frequently can lead to more efficient data gathering. However, it also incurs more overhead for information exchange, which bring extra energy cost for communication and computation to obtain optimal data sensing and data transmission strategies. According to Lemma 3, all the sensors will consume all the allocated energy, means that if the energy allocation changes, the optimal data sensing and data transmission under BEAS will change. Since too much extra energy cost may lead to the decrease of network performance, we need to consider the trade-off between the extra energy cost (for communication and computation) and network utility when updating the energy allocation.

Assume that the energy cost for communication and computation for sensor i to obtain the optimal data gathering is given by a constant ξ_i. If one sensor needs to change its energy allocation, the extra energy cost for sensor in the network will be increased by ξ_i, which is called extra energy cost in the following sections. If the sensors employ BEAS, which does not take the extra energy cost into consideration, they may incur too much extra energy cost, which decreases network performance. Even worse, sensors may run out of energy at some slots.

For **Case I** (see its details in Section IV), the sensors does not need to change their energy allocation. For **Case II** and **III**, the sensors should make decisions whether to change their energy allocation or not according to the values of available energy and extra energy cost. If the extra energy cost is very high, the network performance may be worse than that before. So we propose an improved BEAS according to the value of ξ_i and available energy, given as follows:

For **Case II**: $\bar{t}_1(m) \neq 0$: Since BEAS does not take the extra energy cost into consideration, the maximal virtual battery level after the adjustment by BEAS will be lower than the maximal battery level, which increases the average variation of the energy allocation. For the improved BEAS, the energy allocation will be adjusted, according to the values of extra energy cost and battery level, to minimize the average variation of the energy allocation.

$$A_{i,t}(m+1) = \begin{cases} A_{i,t}(m), & t \leq \overleftarrow{t_1}(m), \\ A_{i,t}(m) + \bar{A}_1(m), & \overleftarrow{t_1}(m) < t \leq \bar{t}_1(m), \\ A_{i,t}(m) - \underline{A}_1(m), & \bar{t}_1(m) < t \leq \overrightarrow{t_1}(m), \\ A_{i,t}(m), & \overrightarrow{t_1}^{*}(m) < t \end{cases}$$

where $\bar{A}_1(m) = \frac{[\hat{B}_i^{up}(m) - B_i^{\max} - \xi_i]^+}{\bar{t}_1(m) - \overleftarrow{t_1}(m)}$ and $\underline{A}_1(m) = \frac{[\hat{B}_i^{up}(m) - B_i^{\max}]^+}{\overrightarrow{t_1}(m) - \bar{t}_1(m)}$.

For **Case III**: $\bar{t}_2(m) \neq 0$: Since the total amount of optimal utility is an increasing function of energy allocation and the total amount of utility satisfies (72), the total amount of optimal utility by BEAS will be decreased if $\xi_i \leq (\bar{t}_2(m) - \overleftarrow{t_2}(m) - 1)\hat{B}_i^{low}(m) - \varsigma$ and ς, where $\varsigma \geq 0$, is a parameter determined by the function of $U(x)$, $\hat{B}_i^{low}(m)$ and ξ_i. Thus, the energy allocation will be changed only if

$$\sum_{t=\overleftarrow{t_2}(m)}^{t=\overrightarrow{t_2}(m)} \sum_i U(X_i(t)) + \sum_i (U(X_i(\bar{t}_2(m))) - U(X_i''(\bar{t}_2(m)))) < \sum_{t=\overleftarrow{t_2}(m)}^{t=\overrightarrow{t_2}(m)} \sum_i U(X_i'(t))$$

where $X(t)$ is the optimal solution for $A(t)$, $X'(t)$ is the optimal solution for $A(t) + \frac{\hat{B}_i^{low}(m) - \xi_i}{\bar{t}_2(m) - \overleftarrow{t_2}(m)}$ and $X''(t)$ is the optimal solution for $A(t) + \hat{B}_i^{low}$, and the improved energy allocation scheme can be given as follows:

$$A_{i,t}(m+1) = \begin{cases} A_{i,t}(m), & t \leq \overleftarrow{t_2}(m), \\ A_{i,t}(m) + \bar{A}_2(m), & \overleftarrow{t_2}(m) < t \leq \bar{t}_2(m), \\ A_{i,t}(m) - \underline{A}_2(m), & \bar{t}_2(m) < t \leq \overrightarrow{t_2}(m), \\ A_{i,t}(m), & \overrightarrow{t_2}(m) < t \end{cases}$$

where $\bar{A}_2(m) = \frac{\hat{B}_i^{low}(m) - \xi_i}{\bar{t}_2(m) - \overleftarrow{t_2}(m)}$ and $\underline{A}_2(m) = \frac{\hat{B}_i^{low}(m)}{\overrightarrow{t_2}(m) - \bar{t}_2(m)}$.

D. Topology Control Scheme

So far, when all the logical links between the sensors are available and the transmit energy consumption matrix are predetermined by Lemma 4, the optimization problem can be solved by the DSR2C algorithm based on the improved BEAS.

According to the definition of $h_{ij,t}$, if $h_{ij,t} \neq 0$, sensor i will transmit sensory data to sensor j at slot t, and the total amount of the data transmitted by link (i,j) is $f_{i,t}^{out} * h_{ij,t}$. Otherwise, the sensor will not transmit any sensory data to sensor j through link (i,j) at slot t.

In optimization problem (41), the sensor i should communicate with sensor j, satisfying $\{j|R_{ij} = 1\}$ and collect information from these sensors, to determine whether transmit/relay sensory data to sensor j or not. Hence, sensor i needs exchange information with sensor j in despite of $h_{ij,t} = 0$, which involves large overhead. In order to decrease unnecessary network overhead, we design a topology control scheme to decrease the message exchange by deactivating the unused established logical links, and activating them again when needed. Typically, the computational complexity for the sensor can be treated as increasing function of number of sensors that it communicates with. Since decreasing the number of sensor's logical links will decrease the number of sensors that it will communicate with,

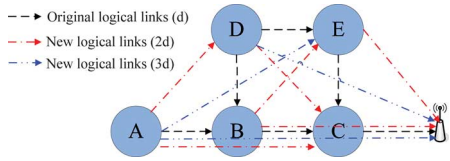

Fig. 3. Network topology.

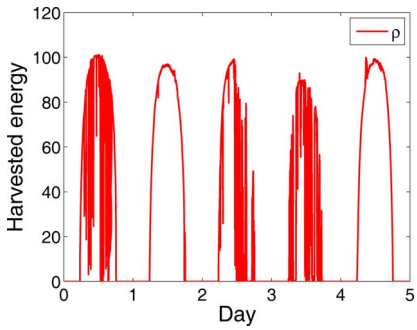

Fig. 4. Experimental data of solar panels obtained from BMS for a period from Sep. 4th to Sep. 8th, 2012.

topology control scheme can reduce the computational complexity.

Initially, the sensors establish all the available logical links to calculate the optimal data sensing and data transmission. When the optimal data sensing and data transmission are obtained by the DSR2C for the first slot, the transmit power control scheme for the next slot can be designed by deactivating the established logical links or activating new logical links as follows:

1) Deactivating:

$$R' = \begin{cases} R'_{ij} = R_{ij}, & \text{if } h_{ij,t} \neq 0, \\ R'_{ij} = 0, & \text{else} \end{cases} \tag{74}$$

deactivating action means that the logical link (i, j) will not be established between sensor i and sensor j to calculate the optimal data sensing and data transmission. Thus, sensor i and sensor j do not need to communicate with each other directly, which can reduce information exchange between them. The goal of the deactivating action is to decrease the unnecessary information exchange for the sensors, which has no direct data transmission between them.

2) Activating:

$$R' = \begin{cases} R'_{ij} = R_{ij}, & \text{if } P_{i,t} < A_{i,t} \text{ and } P_{j,t} < A_{j,t}, \\ R'_{ij} = R'_{ij}, & \text{else.} \end{cases} \tag{75}$$

Activating action means that if one of the sensors between the logical link (i, j) does not use all of the allocated energy, the logical link (i, j) will be established to calculate the optimal data sensing and data transmission, since the remaining energy has the potential to increase the network performance. Thus, the sensors will not miss any opportunity to improve the network performance.

V. Performance Evaluation

In this section, numerical results are shown to demonstrate the performance of proposed algorithms over the existing algorithms. All the results are obtained by MATLAB.

TABLE III
Network Parameter Values

solar panel	$37 \times 33mm^2$	β	0.0108J/kb
B_{max}	304mWh (1094.4J)	μ	0.0002
α[31]	3.14	e^{re}/e^{sn}	0.9936/0.0792J/kb

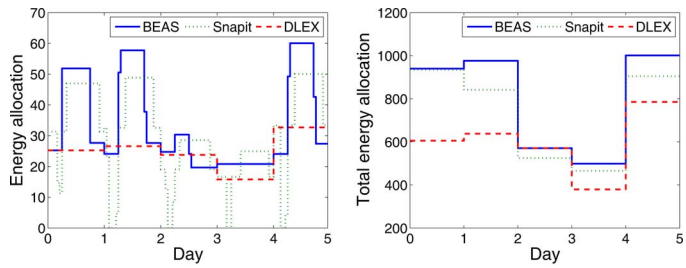

Fig. 5. Energy allocation for sensor C under BEAS, QuickFix with SnapIt and DELX, respectively. (a) Energy allocation. (b) Total energy allocation.

A. Simulation Setting

Fig. 3 shows the network topology for simulation, in which the distance between every two neighboring sensors is $d = 10$ m and (d) denotes the maximal transmission distance d (similar to $(2d)$ and $(3d)$). All the sensors have the same wireless module, such as TelosB from Crossbow [25]. The values of network parameters are given in Table III. Fig. 4 presents the solar profile obtained from baseline measurement system (BMS) of Solar Radiation Research Laboratory (SRRL) for a period from Sep. 4th to Sep. 8th, 2012 [32]. The total amount of harvested energy for the five days are 939.77 mWh, 976.39 mWh, 570.74 mWh, 498.62 mWh and 1001.31 mWh, respectively. Let the initial energy of the rechargeable battery for all senors be 140mWh (504J), and the utility function be $U(x_{i,t}) = \log(x_{i,t})$.

The proposed algorithms are compared with QuickFix with SnapIt in [17], where $\delta = 0.2x_i$, and DLEX [12]. QuickFix calculates the optimal sensing rate using the average energy harvesting rate $\pi_{i,t}$ (see (18)) for each cycle, and SnapIt adapts the sensing rate with the goal of maintaining the battery at a desired level. DELX is designed to compute an optimal lexicographically data collection rate and routing path for each sensor such that no sensor will run out of energy.

B. Performance Evaluation of BEAS

Fig. 5 depicts the results of energy allocation at each slot and total amount of energy allocation during each day for sensor C under BEAS, QuickFix with SnapIt and DELX, respectively. It can be observed that sensor C under QuickFix with SnapIt runs out of energy at some slots, which means that sensor C at these slots stops working. Also, it can be found that the values of allocated energy by BEAS are much larger than that by QuickFix with SnapIt or DLEX at most slots. From Fig. 5(b), it can be seen that the total amount of allocated energy for sensor C under BEAS during the five days are much higher than that under QuickFix with SnapIt or DLEX, especially for the second and fifth days. The simulation results demonstrate the efficiency of our BEAS, especially when the battery capacity is deficient to store all the harvested energy.

TABLE IV
NETWORK UTILITY FOR EACH DAY

Approach	Total Network Utility				
	First Day	Second Day	Third Day	Fourth Day	Fifth Day
DSR2C(d)	332.65	334.92	277.63	263.34	337.028
DSR2C(2d)	405.82	408.09	350.80	336.51	410.20
DSR2C(3d)	413.11	415.38	358.09	343.80	417.48
QuickFix with SnapIt	332.11	$-\infty$	$-\infty$	$-\infty$	$-\infty$
DLEX	286.57	292.89	279.55	230.46	317.86

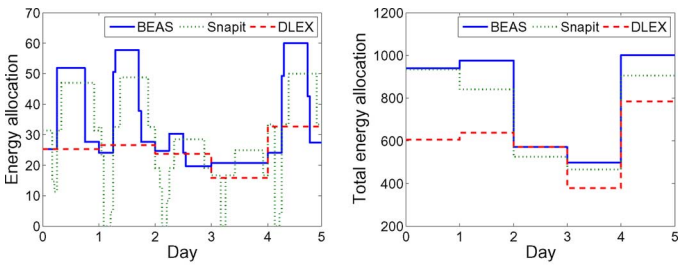

Fig. 6. Battery level and surplus variables for sensor C under BEAS, QuickFix with SnapIt and DELX, respectively. (a) Battery level. (b) Surplus variable.

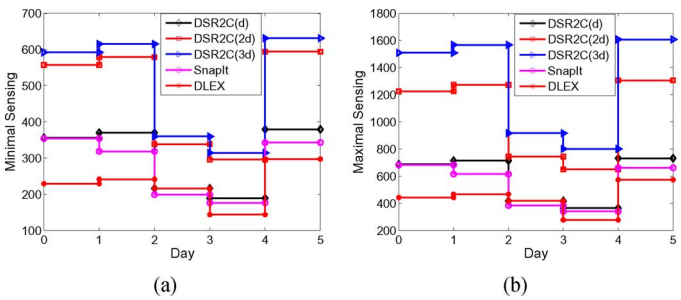

Fig. 7. Total amount of minimal and maximal sensing for each day under DSR2C, QuickFix with SnapIt and DLEX, respectively. (a) Minimal sensing rate. (b) Maximal sensing rate.

Fig. 6 illustrates the battery level and surplus variables $o_{C,t}$ for sensor C under BEAS, QuickFix with SnapIt and DLEX, respectively. As shown in Fig. 6(a), the battery level for sensor C under QuickFix with SnapIt reaches zero at some consecutive slots, which means that sensor C has run out of energy and cannot provide data service at these slots. From Fig. 6(b), it can be seen that sensor C under QuickFix with SnapIt or DLEX cannot store all the harvested energy in the rechargeable battery due to the limited battery capacity, and that under BEAS can reserve all of the harvested energy. Since the harvested energy can be reserved to power the sensor for providing data service, thus the sensor under BEAS has more potential to improve the network performance than that under other two approaches.

C. Performance Evaluation of DSR2C

Minimal and maximal sensing rate usually are used to demonstrate the weakest and strongest performance of the network, so the total amount of minimal and maximal sensing for each day are shown in Fig. 7. It can be found that when the maximal transmission distance is d, sensors under DSR2C obtain highest total amount of minimal and maximal sensing among DSR2C, QuickFix with SnapIt and DLEX, respectively. Moreover, with the increasing of maximal transmission distance, the total amount of minimal and maximal sensing for sensors under DSR2C increases.

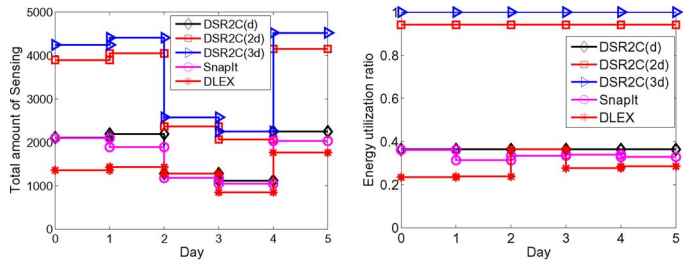

Fig. 8. Total amount of sensory data and energy utilization ratio for each day under DSR2C, QuickFix with SnapIt and DLEX, respectively. (a) Total amount of sensory data. (b) Energy utilization ratio.

The total amount of sensory data and energy utilization ratio for each day are shown in Fig. 8(a). When the maximal transmission distance is d, sensors under DSR2C achieve the highest total amount of sensory data for each day among DSR2C, QuickFix with SnapIt and DLEX, respectively. With the increasing of maximal transmission distance, the total amount of sensory data obtained by sensors under DSR2C increases. Generally, larger amount of sensory data means better network performance. From Fig. 8(b), it can be easily found that sensors under DSR2C with maximal transmission distance $3d$ can best utilize the harvested energy, since all of the harvested energy has been spent. With the decreasing of maximal transmission distance, the energy utilization ratio decreases. When the maximal transmission distance is d, sensors under DSR2C can better utilize the harvested energy than those under QuickFix with SnapIt or DELX. Thus, sensors under DSR2C obtain best performance among those under these three algorithms, which demonstrates the efficiency of DSR2C.

Table IV exhibits the results of network utility for each day. It can be seen that sensors under DSR2C (3d) obtain the highest network utility for each day. Note that the utility obtained by sensors under QuickFix with SnapIt drops to negative infinity except the first day, because sensors under QuickFix with SnapIt run out of energy and stop working at some slots during these days. Moreover, when the maximal transmission distance is d, the overall network utility of the five days obtained by sensors under DSR2C is larger than those under other two algorithms. All these demonstrate that the performance of DSR2C is better than that of other two algorithms.

In summary, simulation results show that the network performance can be increased by adjusting the transmit energy consumption of each sensor to establish new logical links for routing selection. Furthermore, energy utilization ratio can be improved by adjusting transmit energy consumption and selecting optimal sensing rate and routing.

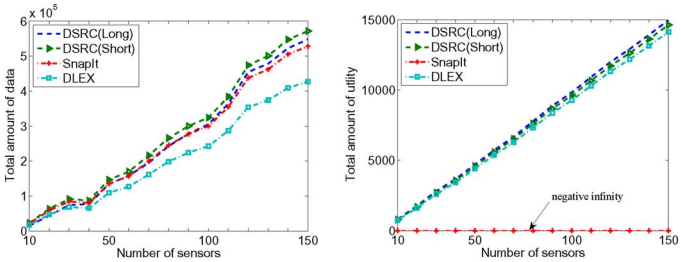

(a) (b)

Fig. 9. The average amount of data and utility during the five days. (a) The average amount of data. (b) The average amount of utility.

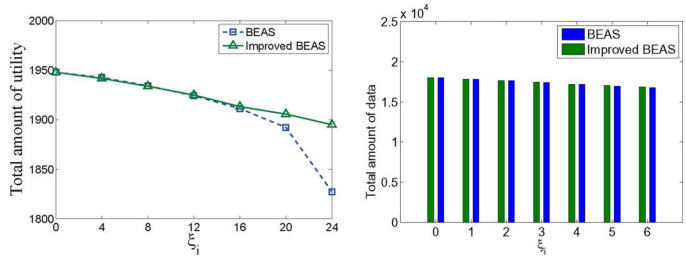

(a) (b)

Fig. 10. Total amount of utility and total amount of data. (a) Total amount of utility. (b) Total amount of data.

D. Performance Evaluation of DoSR for Large Rechargeable Sensor Network

In order to understand the performance of DoSR in large rechargeable sensor networks, we perform simulations in a 200m $\times$ 200 m area, in which sink node is located at $(100, 100)$ and and n, $n = \{10, 20, 30, \ldots, 140, 150\}$, sensors are deployed into this area randomly. The simulation results can be found in the Fig. 9, where *Long* means that the maximal transmission distance for each sensor is 150 m and *Short* means that the maximal transmission distance for each sensor, which is the same as that set by QuickFix with SnapIt or DLEX, is 60 mm.

It can be found that with the increase of the number of sensors, the total amount of data, as well as the total amount of utility increases. Also, it can be seen from that DSRC (Long) obtains the highest average amount of utility while DSRC (Short) obtains the highest average amount of data. Combined with the simulation results in Table IV, we observe that similar conclusions can be made by comparison with the simulation settings where small number of sensors are used.

E. Performance Evaluation of Improved BEAS

In this section, simulation results under BEAS and improved BEAS are given to demonstrate the efficiency of the proposed algorithms. Fig. 10 shows the relationship between the ξ_i and the total amount of utility. It can be found that the total amount of the utility will be decreased with the increase of extra energy cost. More important, the total amount of utility for the sensors under BEAS decreases faster than that under improved BEAS. It can be seen from Fig. 10(b) that the difference of the total amount of the data for the sensors under BEAS and improved BEAS is very small, but difference of the total amount of utility is much larger. That is because the improved BEAS can maximize the total amount of data while keeping the fairness of networks. Thus, improved BEAS can deal with the extra energy cost to maximize the total amount of utility.

F. Performance Evaluation of Topology Control Scheme

We use the values of sensing rates $\boldsymbol{x}$ for each iteration to demonstrate the convergence rate of DSR2C with or without topology control scheme, when maximal transmission distance is $3d$. The simulation results are shown in Fig. 11. It can be found that the sampling rates under DSR2C with or without topology control scheme have the similar convergence rate. Table V shows the change of accessible matrix R when the topology control is added to the DSR2C. The sensor under

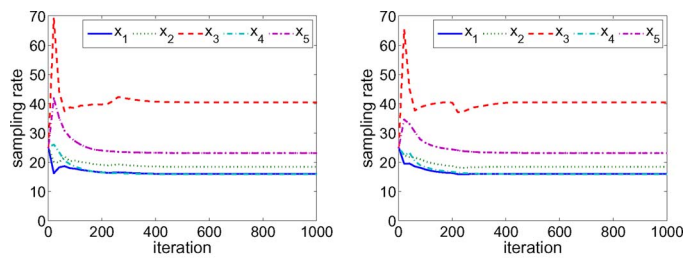

(a) (b)

Fig. 11. Convergence of the DSR2C with or without topology control. (a) With topology control. (b) Without topology control.

TABLE V
CHANGE OF R FOR ADDING TOPOLOGY CONTROL TO DSR2C

	$R_{:A}$	$R_{:B}$	$R_{:C}$	$R_{:D}$	$R_{:E}$	$R_{:S}$
$R_{A:}$	0	1	$1 \to 0$	$1 \to 0$	$1 \to 0$	1
$R_{B:}$	0	0	1	0	$1 \to 0$	1
$R_{C:}$	0	0	0	0	0	1
$R_{D:}$	0	$1 \to 0$	1	0	1	1
$R_{E:}$	0	0	$1 \to 0$	0	0	1
$R_{S:}$	0	0	0	0	0	0

DSR2C should communicate with a certain number of sensors defined by accessible matrix R to compute optimal data sensing and routing. It can be found that topology control scheme can reduce the communication between the sensors in an efficient way. For example, without topology control scheme, sensor A should communicate with sensors B, C, D, E and sink node S, but with topology control, sensor A only needs to communicate with sensor B and sink node S. Thus, DSR2C with topology control can reduce computational complexity while it will not affect convergence of the algorithm.

VI. CONCLUSION

In this paper, we have studied dynamic sensing and routing problem to maximize overall network utility for rechargeable sensor networks. We first proposed a balanced energy allocation scheme (BEAS) to manage energy use for each sensor as smooth as possible. By introducing flow variables to simplify the relationship between sensing rates and flow rates, we developed a distributed sensing rate and routing control (DSR2C) algorithm to obtain the optimal sensing rate and routing by employing theory of dual decomposition while taking the dynamic feature of network topology into account. An improved BEAS was proposed by taking extra energy cost into consideration to manage the energy allocation and a topology control scheme

was proposed to reduce computational complexity. Extensive simulation results are given to demonstrate the efficiency of our algorithms by comparing with existing algorithms.

REFERENCES

[1] S. Lindsey, C. Raghavendra, and K. M. Sivalingam, "Data gathering algorithms in sensor networks using energy metrics," *IEEE Trans. Parallel Distrib. Syst.*, vol. 13, no. 9, pp. 924–935, 2002.

[2] G. Lu, B. Krishnamachari, and C. S. Raghavendra, "An adaptive energy-efficient and low-latency MAC for tree-based data gathering in sensor networks," *Wireless Commun. Mobile Comput.*, vol. 7, no. 7, pp. 863–875, 2007.

[3] K. Lin *et al.*, "Heliomote: enabling long-lived sensor networks through solar energy harvesting," in *Proc. ACM SenSys*, 2005, pp. 309–309.

[4] C. Park and P. Chou, "Ambimax: Autonomous energy harvesting platform for multi-supply wireless sensor nodes," in *Proc. IEEE SECON*, Reston, VA, USA, 2006, pp. 168–177.

[5] S. He, J. Chen, F. Jiang, D. Yau, G. Xing, and Y. Sun, "Energy provisioning in wireless rechargeable sensor networks," *IEEE Trans. Mobile Comput.*, vol. 12, no. 10, pp. 1931–1942, 2013.

[6] L. He *et al.*, "Esync: An energy synchronized charging protocol for rechargeable wireless sensor networks," *Proc. ACM Mobihoc*, pp. 247–256, 2014.

[7] C. Hua and T. S. P. Yum, "Optimal routing and data aggregation for maximizing lifetime of wireless sensor networks," *IEEE/ACM Trans. Netw.*, vol. 16, no. 4, pp. 892–903, 2008.

[8] S. He, J. Chen, D. K. Y. Yau, and Y. Sun, "Cross-layer optimization of correlated data gathering in wireless sensor networks," *IEEE Trans. Mobile Comput.*, vol. 11, no. 11, pp. 1678–1691, 2012.

[9] L. Chen, S. H. Low, and J. C. Doyle, "Cross-layer design in multihop wireless networks," *Comput. Netw.*, vol. 55, no. 2, pp. 480–496, 2011.

[10] J. Chen *et al.*, "Utility-based asynchronous flow control algorithm for wireless sensor networks," *IEEE J. Sel. Areas Commun.*, vol. 28, no. 7, pp. 1116–1126, 2010.

[11] Y. Liu, A. Liu, and Z. Chen, "Analysis and improvement of send-and-wait automatic repeat-request protocols for wireless sensor networks," *Wireless Personal Commun.*, pp. 1–37, 2014.

[12] R. S. Liu, K. W. Fan, Z. Z. Zheng, and P. Sinha, "Perpetual and fair data collection for environmental energy harvesting sensor networks," *IEEE/ACM Trans. Netw.*, vol. 19, no. 4, pp. 947–960, 2011.

[13] J. Nair and D. Manjunath, "Distributed iterative optimal resource allocation with concurrent updates of routing and flow control variables," *IEEE/ACM Trans. Netw.*, vol. 17, no. 4, pp. 1312–1325, 2009.

[14] C. Long, B. Li, Q. Zhang, B. Zhao, B. Yang, and X. Guan, "The end-to-end rate control in multiple-hop wireless networks: cross-layer formulation and optimal allocation," *IEEE J. Sel. Areas Commun.*, vol. 26, no. 4, pp. 719–731, 2008.

[15] Y. Xi and E. M. Yeh, "Node-based optimal power control, routing, and congestion control in wireless networks," *IEEE Trans. Inf. Theory*, vol. 54, no. 9, pp. 4081–4106, 2008.

[16] S. Chen, P. Sinha, N. B. Shroff, and C. Joo, "A simple asymptotically optimal energy allocation and routing scheme in rechargeable sensor networks," in *Proc. IEEE INFOCOM*, 2012, pp. 379–387.

[17] R. S. Liu, P. Sinha, and C. E. Koksal, "Joint energy management and resource allocation in rechargeable sensor networks," in *Proc. IEEE INFOCOM*, San Diego, CA, USA, 2010, pp. 1–9.

[18] L. Lin, N. B. Shroff, and R. Srikant, "Asymptotically optimal energy-aware routing for multihop wireless networks with renewable energy sources," *IEEE/ACM Trans. Netw.*, vol. 15, no. 5, pp. 1021–1034, 2007.

[19] C. Zhang, J. Kurose, Y. Liu, D. Towsley, and M. Zink, "A distributed algorithm for joint sensing and routing in wireless networks with non-steerable directional antennas," in *Proc. IEEE ICNP*, 2006, pp. 218–227.

[20] V. Joseph, V. Sharma, U. Mukherji, and M. Kashyap, "Joint power control, scheduling and routing for multicast in multihop energy harvesting sensor networks," in *Proc. ICUMT*, 2009, pp. 1–8.

[21] M. Zhao, J. Li, and Y. Yang, "Joint mobile energy replenishment and data gathering in wireless rechargeable sensor networks," in *Proc. ITC*, 2011, pp. 238–245.

[22] X. Jiang, J. Polastre, and D. Culler, "Perpetual environmentally powered sensor networks," in *Proc. IPSN*, 2005, pp. 463–468.

[23] A. Kansal, J. Hsu, S. Zahedi, and M. B. Srivastava, "Power management in energy harvesting sensor networks," *ACM Trans. Embedded Comput. Syst. (TECS)*, vol. 6, no. 4, 2007, Article No. 32.

[24] D. K. Noh and K. Kang, "Balanced energy allocation scheme for a solar-powered sensor System and its effects on network-wide performance," *J. Comput. Syst. Sci.*, vol. 77, no. 5, pp. 917–932, 2011.

[25] K. W. Fan, Z. Z. Zheng, and P. Sinha, "Steady and fair rate allocation for rechargeable sensors in perpetual sensor networks," in *Proc. ACM SenSys*, New York, NY, USA, 2008, pp. 239–2528.

[26] Y. Zhang *et al.*, "Distributed sampling rate control for rechargeable sensor nodes with limited battery capacity," *IEEE Trans. Wireless Commun.*, vol. 12, no. 6, pp. 3096–3106, 2013.

[27] J. Pan, Y. T. Hou, L. Cai, Y. Shi, and S. X. Shen, "Topology control for wireless sensor networks," *Proc. ACM MobiCom*, pp. 286–299, 2003.

[28] Z. Wang, J. Liao, Q. Cao, H. Qi, and Z. Wang, "Achieving k-barrier coverage in hybrid directional sensor networks," *IEEE Trans. Mobile Comput.*, vol. 13, no. 7, pp. 1443–1455, 2014.

[29] S. H. Low and D. E. Lapsley, "Optimization flow control–I: Basic algorithm and convergence," *IEEE/ACM Trans. Netw.*, vol. 7, no. 6, pp. 861–874, 1999.

[30] M. Chiang, "Balancing transport and physical layers in wireless multihop networks: Jointly optimal congestion control and power control," *IEEE J. Sel. Areas Commun.*, vol. 23, no. 1, pp. 104–116, 2005.

[31] B. Gaudette, V. Hanumaiah, S. Vrudhula, and M. Krunz, "Optimal range assignment in solar powered active wireless sensor networks," in *Proc. IEEE INFOCOM*, 2012, pp. 2354–2362.

[32] Baseline Measurement System (BMS), NREL Solar Radiation Research Lab. [Online]. Available: www.nrel.gov/midc/srrl_bms/

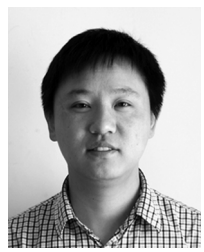

Yongmin Zhang (S'12) received the Ph.D. degree in control science and engineering from Zhejiang University, Hangzhou, China, 2015.

From November 2013 to June 2014, he was a visiting scholar with the California Institute of Technology, Pasadena, CA, USA. He is a member of the Group of Networked Sensing and Control (IIPC-NeSC) in the State Key Laboratory of Industrial Control Technology at Zhejiang University. His research interests include wireless sensor networks and smart grid.

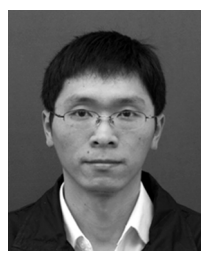

Shibo He (M'13) received the Ph.D. degree in control science and engineering from Zhejiang University, Hangzhou, China, in 2012.

From November 2010 to November 2011, he was a visiting scholar with the University of Waterloo, Waterloo, ON, Canada. He was an associate research scientist from March 2014 to May 2014, and a Postdoctoral Scholar from May 2012 to February 2014, both with Arizona State University, Phoenix, AZ, USA. He is currently a Research Professor at Zhejiang University. His research interests include wireless sensor networks, crowd sensing, and big data analysis. He currently serves on the editorial board of Springer *Peer-to-Peer Networking and Application*, and is a guest editor of Elsevier *Computer Communications* and *Hindawi International Journal of Distributed Sensor Networks*.

Jiming Chen (M'08–SM'11) received the B.Sc. and Ph.D. degrees, both in control science and engineering, from Zhejiang University, China, in 2000 and 2005, respectively.

He was a visiting researcher at INRIA in 2006, National University of Singapore in 2007, and University of Waterloo from 2008 to 2010. Currently, he is a full Professor with the Department of Control Science and Engineering, and the coordinator of the group Networked Sensing and Control in the State Key Laboratory of Industrial Control Technology, Vice Director of Institute of Industrial Process Control at Zhejiang University, China. His research interests include sensor networks and networked control.

Dr. Chen currently serves as an associate editor for several international journals including IEEE TRANSACTIONS ON PARALLEL AND DISTRIBUTED SYSTEMS, IEEE *Network*, and IEEE TRANSACTIONS ON CONTROL OF NETWORK SYSTEMS. He was a guest editor of IEEE TRANSACTIONS ON AUTOMATIC CONTROL and others.